Journal of the Air Transport Research Society 3 (2024) 100036

Contents lists available at ScienceDirect

Journal of the Air Transport Research Society

journal homepage: www.elsevier.com/locate/jatrs

The integration of En route flow optimization, complex network clustering, and rule-based approach to airspace sub-sectorization for enhanced air traffic monitoring

Aitichya Chandra, M.E, Ph.D. Student[a], Sayan Hazra, M.Sc[b], Ashish Verma, PhD, Professor[a,*]

[a] Department of Civil Engineering, Indian Institute of Science (IISc) Bangalore, Bangalore, Karnataka, India, 560012
[b] Department of Computer Science and Engineering, Pondicherry University, Puducherry, India, 605014

ARTICLE INFO

Keywords:
Air traffic monitoring
En route flow optimization
Airspace sectorization
Complex network clustering
Multi-objective optimization

ABSTRACT

This study proposes the use of a novel integrated framework for 2D en route airspace sub-sectorization. The integrated framework combines the multi-commodity flow optimization approach, complex network clustering approach, and Minimum Bounding Geometry (MBG)-coupled Rule-based Approach for boundary design. A decomposition-based discrete particle swarm optimization (DPSO) is used to solve the clustering problem. The output of the flow optimization is used as a guiding standard for the DPSO. Experimentations were performed using the Indian airspace sector to validate the framework and DPSO was run for different maximum number of generations ($maxgen$). The findings reveal that the multi-commodity flow approach captures system-wide flow operations. Clustering results corresponding to $maxgen = 100$ and $maxgen = 150$ perform best in terms of equitable and balanced distribution of cluster size and traffic load. The MBG-coupled Rule-based Approach leads to compact and convex sub-sector boundary design. Major implications of this research include dynamic adaptability of the integrated framework, increased sensitivity of sector design to network evolution, and a computationally tractable framework. The higher controllability of the proposed framework also offers an increased acceptance among practitioners.

1. Introduction

Airspace sectors are a fundamental feature of the air traffic management (ATM) system. Sectors are smaller partitions in the airspace, monitored by a team of controllers to ensure better traffic monitoring and coordination (Teixeira 2015; Yin et al., 2017). Efficient sector organisation leads to balanced workload distribution, subsequently contributing to smooth coordination between sectors, reduced flight re-routing, enhanced operational flexibility, and better ATM performance (Jakšić and Janić 2020; Janić 1997; Mogtit et al. 2020Zou et al. 2016;). With increased demand, sector flow increases, affecting sector organisations. Sub-optimal sector design leads to an imbalanced distribution of workload among controllers, exerting significant delays and safety concerns (Teixeira, 2015). Imbalanced workload distribution has imminent effects on aviation safety and the controller's situation awareness (van de Merwe et al. 2012; Milan, 1989), reducing operations efficiency. As a result, systematic airspace partitioning and design techniques are crucial to an ATM system (Gianazza 2017; Kulkarni et al., 2011; Lee et al. 2010; Li et al. 2009). The complete task has been identified as the airspace sectorization problem in ATM literature.

The airspace sectorization problem is an intriguing, non-trivial problem with conflicting objectives and network and geometric constraints (Jagare et al., 2013; Tang et al. 2012). The primary criteria for designing airspace sectors include (Li et al. 2009; Mogtit et al. 2020; Tang et al. 2012; Teixeira 2015; Zou et al. 2016): (i) Workload: Sector traffic load should be within an acceptable threshold (ii) Convexity: Sectors should not be irregularly shaped; (iii) Boundary: Sector boundary should have a minimum distance from the potential point of conflicts and waypoints and (iv) Connectivity: Sectors should be contiguous and not fragmented. Literature highlights multiple approaches to the airspace sectorization problem. The problem can be two-dimensional (2D) or three-dimensional (3D), static or dynamic (Kopardekar et al., 2007). The underlying complexity has attracted extensive research efforts ranging from geometry-based to graph-based approaches (Flener and Pearson 2013; Li et al. 2010; Li et al. 2009; Mogtit et al. 2020; Sergeeva et al. 2015; Sergeeva et al. 2017). Different approaches generate different sector configurations with unique advantages and disadvantages.

This study limits it to the two-dimensional (2D) static en route sectorization problem (2D ERSP), where sectors are partitioned in the horizon-

* Corresponding author
E-mail addresses: aitichyachandraofficial@gmail.com (A. Chandra), sayanrik1996@outlook.com (S. Hazra), ashishv@iisc.ac.in (A. Verma).

https://doi.org/10.1016/j.jatrs.2024.100036
Received 30 May 2024; Received in revised form 29 July 2024; Accepted 30 July 2024
2941-198X/

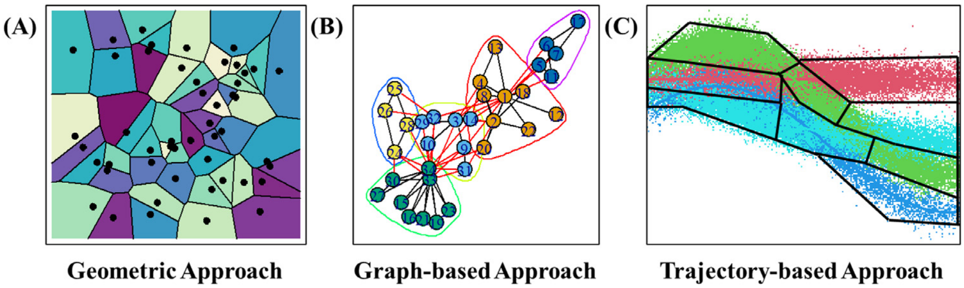

Fig. 1. Indicative sketch of the three major sector design approaches.

tal plane. The 2D ERSP is typically posed as a multi-objective problem, aiming to minimise intrasector and intersector workload while ensuring the primary constraints such as connectivity, convexity, and sector overload (Zou et al., 2016). Within the research domain addressing the 2D ERSP, four critical avenues remain largely unexplored: the subdivision of sectors into sub-sectors for enhanced granularity, addressing the system-wide flow operations, addressing complex air traffic network behaviour through network clustering principles, and the possibility of a thumb rule for convex and compact boundary design. This study aims to tackle these avenues by investigating the validating of an integrated framework of system-wide network optimization, complex network clustering, and rule-based boundary design to model and solve the airspace sub-sectorization task. The primary motivation for this research effort is aimed at improving the overall ATM efficiency and resilience.

It is worth noting that Trajectory Based Operations (TBO) are expected to be a new ATM paradigm with substantial interest from diverse stakeholders (Gardi et al., 2019; Rosenow et al., 2021; Sáez et al., 2020; Wandelt and Sun, 2014). Hence, a question naturally arises on the relevance of this study in the given context. Literature indicates that trajectory efficiency in terms of the difference between the actual flight path and the shortest path (great circle distance) often depends on the en route sector shape, size, design, and route configuration (Rosenow et al., 2021). Recent studies have emphasized the interplay of optimal 2D en route sectors with 4D trajectory analysis and optimization. The highlights include the (i) role of en route segments on the horizontal trajectory shape that influences the design of optimal alternative routes for 4D trajectories (Dai et al., 2019; Juntama, 2022) and (ii) the importance of equitable controller task load in trajectory optimization (Zeh et al., 2024). Furthermore, 2D static en route sector designs have proved useful in ATM sub-problems such as horizontal conflict detection, airspace efficient analysis in the presence of TBO, initial planning tool for optimal 4D TBO, airspace congestion, and simplified management of low-density airspace (Airports Authority of India, 2018; Cai et al. 2017; Dai et al. 2019; Gardi et al., 2019; Guan et al. 2017; Juntama 2022; Zeh et al. 2024). Hence, even after the evolution of sophisticated TBO frameworks, the 2D ERSP remains valuable for both specific en route management applications and 4D TBO research.

The rest of the paper is structured as follows. The next section highlights the background and research rationale to address the problem. Section 3 discusses the overall research design, including the frameworks for network optimization, clustering, and sub-sector boundary design. Section 4 describes the experimental setup to implement and validate the proposed framework. Section 5 explains the results, followed by the discussions on research implications and limitations in Section 6. The final section, Section 7, summarises and concludes the study.

2. Research background and rationale

Various techniques have been employed to address the 2D ERSP. One of the earliest investigations was conducted by Delahaye et al. (Delahaye et al. 1994), utilising genetic algorithms to generate optimal sector configurations. Subsequent research advancements in addressing the problem can be classified into three categories (Leiden et al., 2009; Mogtit et al. 2020; Zou et al. 2016): (i) geometry-based or region-based approaches utilising Voronoi diagrams coupled with Evolutionary Algorithms (EAs) to design sectors, (ii) weighted undirected graph cutting approaches coupled with EAs to partition airspace graphs into sub-graphs i.e. sectors, and (iii) trajectory clustering approaches coupled with cell (grid) growth (grouping) techniques to design sectors around major routes. An indicative sketch of the three approaches are provided in Fig. 1. All three sketches, 1A, 1B, and 1C, are generated in R using the “deldir”, “igraph”, and “trajectories” packages, respectively. Each approach offers specific advantages in handling the problem’s complexity but also exhibits unique limitations. Geometry-based or region-based methods are popular, flexible, and easy to build but computationally expensive, struggle to achieve workload balance and represent the air-route structure efficiently (Xue 2009; Tang et al. 2012; Xue 2010; Hind et al. 2018; Yousefi 2005). The weighted graph-cutting approaches are promising in addressing complex objectives and representing the underlying topology of the airspace but have limited adaptability to the 3D problem and struggle with boundary design and convexity (Chen and Zhang 2014; Hind et al. 2018; Li et al. 2009; Li et al. 2010;). Trajectory clustering approaches are the most flexible approach but may encounter challenges in compact shape generation and trajectory prediction (Brinton and Pledgie, 2008; Jagare et al., 2013; Hind et al. 2018).

Table 1 presents selected research studies dealing with the 2D ERSP. The table summarizes the problem objective(s), constraints, methodology, and key takeaway (s). The state-of-the-art clearly reveals that current approaches and existing methods often fail to fully account for the inherent complexities that networks introduce to the problem itself. This translates to a disregard for the intricate interactions and dependencies within the network structure. Second, traffic data is a crucial input, and it is expected that airspace configurations cope with traffic states. However, practically no study considers the implications of network-aware demand-based traffic flow values as input (Hind et al., 2018). Finally, the existing approaches frequently struggle with the challenge of designing smooth, convex, and compact sector boundaries. To reduce computational complexity, some approaches resort to outsourcing the criteria of convexity and compactness as post-processing steps, essentially splitting them from the overall design methodology (Chandra et al., 2024). Hence, despite the substantial advancements in the state-of-the-art, there remain a few critical gaps that motivate continuing research efforts. Further exploration into the state-of-the-art of airspace design and sectorization, as well as a summary of the advantages and disadvantages of different approaches, can be found in Hind et al. (2018).

Based on the comprehensive review, the future avenues of improvements include (i) computationally tractable approaches, (ii) static-to-dynamic and dynamic-to-static adaptability, (iii) reflection of system-wide flow operations, (iv) reflection of inherent network complexities, dynamics, and structures, and (v) thumb rule for convex and compact sector design. The aspects of system-wide flow, inherent network complexities, tractable methods, and thumb rule play critical roles. Literature highlights the importance of system-wide flow assignment on networks in traffic control and sector management (D. Chen et al. 2017; D. Chen et al. 2016; Bianco and Bielli 1992; Pien et al. 2015). The system-wide flow assignment should respect the network capacity con-

Table 1
Summary of selected studies on 2D ERSP.

Author(s)	Objective(s)	Constraints	Methodology	Key Takeaway(s)
Mogtit et al. (2020)	Min CORD	SECT, MIND, CONV, CONC, and BAL	Multi-agent optimization using ordered weighted averaging	Superior solution outcome
Gerdes et al. (2016)	Min BAL	COMP and CORD	Fuzzy clustering, VOR, and EVO	Dynamic adaptability
Todorov and Simeonov (2020)	Min (BAL+ CORD + CONF)	SECT and CONV	VOR and geometric algorithm	Sector size has a lower bound
Zou et al. (2016)	Min (BAL+ CORD+ SECT)	CONV, CONC, INTR, MIND, and COMP	Graph cutting and EVO	Boundary definition using the concave hull
Treimuth et al. (2016)	Min (BAL+INTR+TRA)	CONC and MIND	GRA as MIP solved using branch-and-price	Absence of COMP and CONV consideration
Chen and Zhang (2014)	Min (BAL+CORD)	CONV, CONC, and MIND	GRA and EVO	Low traffic results in fewer sectors
Chen et al. (2013)	Min (BAL+CORD+ SECT)	CONV, MIND, and CONC	GRA and EVO	Inherently warrant COMP
Sherali and Hill (2013)	Min (BAL+ CORD+ CONF)	CONV, MIND, and CONC	Restricted bisection reformulated as MIP	Leveraging convex hull for boundaries
Yang et al. (2022)	Min (INTR+ CORD+ BAL)	SECT, MIND, and CONV	Binar search based GRA	Limitations in boundary design
Savai et al. (2010)	Min (BAL+CORD+TRA+PART)	INTR and CONC	Multilevel GRA	Better BAL
Li et al. (2010)	Min (INTR+ CORD+ CFW)	INTR, CONV, and MIND	GRA and Spectral clustering	Efficient design of boundaries
Xue (2009)	Min (BAL+ CORD +MIND+SECT)	CONV and CONC	VO and EVO	BAL dominates decisions

Notations: CORD- Coordination workload; BAL- Balancing workload; INTR- Intrasector workload; CONF- Conflict workload; TRA- Transition between sector; SECT-Sector-crossing time violation; CONV- Convexity; CONC- Connectivity; MIND- minimum distance between fixes and boundaries; COMP- Compactness; EVO- Evolutionary algorithms; VOR- Voronoi diagrams; GRA- Graph partitioning; MIP- mixed integer programming; PART- Partitioning time.

straints and match the traffic demand. Studies on system-wide network optimization, however, are limited. The majority of efforts hint towards the use of a multi-commodity like flow optimization model, with each Origin-Destination (OD) pair treated as a commodity and represented by a Source (Origin), Sink (Destination), and Demand (Chen et al. 2017; Bianco and Bielli 1992; Pien et al. 2015). Such models have dynamic adaptability and prove useful in improving air traffic management efficiency. Apart from the multi-commodity nature of en route flow, air transportation networks also exhibit complex dynamics akin to social media networks, as evidenced by previous studies (Bagler 2008; Huber 2018; Pien et al. 2015). For instance, the air transportation network in India demonstrates hierarchical traits, with traffic load concentrated on interconnected airports, a pattern expected to intensify with the growth of low-cost air services (Bagler 2008). This hierarchical structure, characterised by a truncated scale-free degree distribution, is not unique to India but is also observed in networks of other countries like Australia and China (Hossain and Alam 2017; Wang et al. 2011). Recent literature., although limited, suggest that it is reasonable to infer similar complex organization in worldwide air transportation networks (Sun, Wandelt, and Zanin 2017; Liu, Wang, and Zhang 2023).

Until now, existing sectorization techniques have overlooked the above-discussed aspects of system-wide flow operations and the inherent complexity of air transportation networks. Furthermore, the sector design has been dealt with differently during the post-processing step, with no common set of rules for compact and convex boundary design (Mogtit et al. 2020; Chandra et al., 2024. A suitable thumb rule is essential to decrease the overall problem complexity of similar tasks (Martínez 2006; Openshaw 1978; Openshaw 1977; L Martinez 2007; Evler et al. 2021). Therefore, by conceptualising an integrated framework involving a complex network clustering problem guided by a system-wide network optimization model, we can leverage the overlooked aspects (Chandra et al., 2024). Further, the utility of network clustering and thumb-rule is definitive in eliminating the need for exclusive connectivity constraints, thereby reducing, and improving the computational tractability of the overall problem.

3. Research Design

The overall research design is illustrated in Fig. 2. The process begins with a directed network graph, considering key characteristics such as edge length and capacity. Subsequently, a network flow optimization model is used to determine the optimal flow on each edge. The total input flow at each vertex is then computed as the summation of flows from all incoming edges connected to that vertex.

Based on the range of all input flow values, we introduce a categorical weighting scheme to classify vertices into high, medium, and Low load categories. Specifically, vertices with total incoming flow within the first tertile of input flow are categorised as *Low* load vertices having a discrete traffic load value of 1. Vertices with total incoming flow within the second tertile of input flow are categorised as *Medium* load vertices having a discrete traffic load value of 2. Lastly, vertices with total incoming flow within the third tertile of input flow are categorised as *High* load vertices having a discrete traffic load value of 3. The graph is then converted into an undirected graph for network clustering, and the vertex labels are used as guides to obtain optimal cluster partitions. The final step involves the application of a Minimum Bounding Geometry (MBG)-coupled Rule-based Approach to design sub-sector boundaries.

3.1. Network Flow Optimization Formulation

Consider the 2D airspace network, $G = (V, E)$ with a set of vertices V and a set of edges E. Here, V represents all potential airports and navigation aids, commonly referred to as waypoints. Correspondingly, the set E encompasses the edges connecting these vertices, symbolising the established air routes within the airspace. Let the capacity of an edge $(a, b) \in E$ be $C_{a,b}$. Let the length/cost (distance measure) of an edge $(a, b) \in E$ be $d_{u,v}$. Assuming the set K of k OD pairs, where an OD pair is defined by a triple- source, sink and demand, i.e., $(s_i,\ t_i,\ d_i)$. Let the decision variable be the flow of OD pair k on the edge $(a, b) \in E$, $f_k(a, b)$. The optimal flow problem can now be formulated as a multi-commodity flow problem (MCFP) where each OD pair is a commodity, and the task is to find the feasible flow of commodity k on edge (a, b) minimising the cost $\sum_{k\in K} \sum_{(a,b)\in E} d_{a,b} f_k(a, b)$. Hence, the flow optimization problem can be formulated as

$$\min_f \left(\sum_{k\in K} \sum_{(a,b)\in E} d_{a,b} f_k(a, b) \right) \tag{1}$$

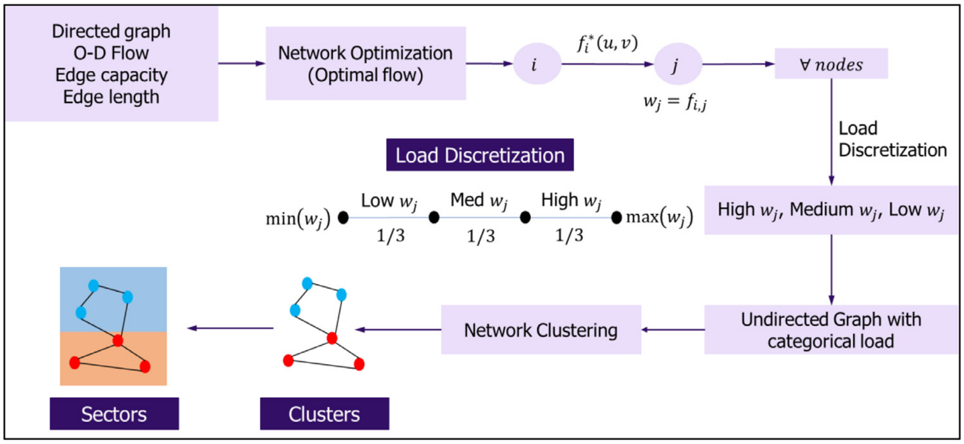

Fig. 2. Overall Research Design.

$s.t.$

$$\sum_{(a,b)\in E} f_k(a,b) - \sum_{(b,a)\in E} f_k(b,a) = \begin{cases} 0, & a \neq s,\ u \neq t \\ d_i, & a = s \\ -d_i, & a = t \end{cases} \quad \forall a \in V,\ k \in K \tag{2}$$

$$\sum_{k\in K} f_k(a,b) \le C_{a,b}\ \forall (a,b) \in E \tag{3}$$

$$f_k(a,b) \ge 0\ \forall k \in K,\ (a,b) \in E \tag{4}$$

Equation 1 aims at minimising the cost of flow. Equation 2 ensures flow conservation at each node. It suggests that for a given OD pair, the flow of that OD pair entering a transit node $a \in V$ is the same as the flow of that OD pair leaving the transit node. Additionally, the demand of that OD pair must exit the source node completely. Simultaneously, the demand of that OD pair must enter the sink node completely. Equation 3 ensures that the sum of flows from all OD pairs on an edge does not exceed the capacity of the edge. Finally, Equation 4 ensures that the flow values are non-negative.

3.2. Complex Network Clustering

Complex network clustering problem is posed as an optimization problem. Given a network represented as $G = (V, E)$, two critical parameters have been proposed in the complex network literature: k-means (KKM) and ratio cut (RC) (Gong, Ma, et al. 2012). Minimising KKM aims to minimise the sum of edge densities within a cluster while minimising RC aims to minimise the sum of edge densities between clusters. For this research, we redefine KKM and RC as Link Density Within Clusters (LDWC) and Link Density Between Clusters (LDBC), respectively. Thus, minimisation of LDWC ensures equitable distribution of intracluster (intra sub-sector) edge densities across different sub-sectors. Conversely, minimising LDBC ensures a balanced distribution of intercluster (inter sub-sector) edge densities. Consequently, the clustering problem is transformed into a multi-objective optimization problem with two objectives.

$$\min \begin{cases} LDWC \\ LDBC \end{cases} \tag{5}$$

Considering that the adjacency matrix A_{ij} carries the vertex adjacency information, and there exists c clusters (subgraphs/partitions) for this network such that $C = \{V_1, V_2, \dots, V_c\}$ where V_i represent the set of vertices in clusters (subgraphs/partitions) G_i and $i = (1, 2, \dots, c)$. Let $|V_i|$ be the number of vertices in the i^{th} cluster and $\bar{V}_i = C - V_i$. The network clustering problem can be solved by ensuring the following objectives are met:

$$\min \begin{cases} LDWC = 2(n-c) - \sum_{i=1}^{c} \left[\frac{\sum_{i\in V_i, j\in V_i} A_{ij}}{|V_i|} \right] \\ LDBC = \sum_{i=1}^{c} \left[\frac{\sum_{i\in V_i, j\in \bar{V}_i} A_{ij}}{|V_i|} \right] \end{cases} \tag{6}$$

It's important to acknowledge that LDWC and LDBC present conflicting objectives. LDWC decreases with an increase in the number of clusters, whereas LDBC increases with the same.

3.2.1. Discrete Particle Swarm Optimization Framework

The approach of employing the decomposition-based discrete particle swarm optimization (DPSO) framework for addressing the multi-objective problem was introduced by Gong et al. (2014). This framework holds several benefits comprising (i) rapid convergence, (ii) automatic determination of the cluster count, (iii) seamless integration with network topology, and (iv) the capability to generate solutions evenly distributed along the Pareto front. Let a particle i be denoted by its position, $X_i = \{x_1, x_2, \dots, x_n\}$ where $x_i \in [1, n]$. Here, n represents the number of vertices. The velocity of particle i is denoted as $V_i = \{v_1, v_2, \dots, v_n\}$ such that,

$$v_i = \begin{cases} 1, & if\ x_i\ changes \\ 0, & otherwise \end{cases} \tag{7}$$

The velocity update rule for a particle i is redefined and is given by

$$V_i = sig\left(\gamma V_i + s_1 z_1 \left(P_{best_i} \oplus X_i\right) + s_2 z_2 \left(G_{best} \oplus X_i\right)\right) \tag{8}$$

$$\gamma, z_1, z_2 \in [0, 1] \tag{9}$$

where γ represents the weight of inertia in PSO. s_1 and s_2 are cognitive and social parameters. z_1 and z_2 are random numbers. Let P_{best_i} be the personal best position of particle i and G_{best} be the global best position of the population. The $\oplus$ is the XOR operator. The function $Z = sig(X)$ where $Z = (z_1, z_2, \dots, z_n)$ is defined as

$$z_i = \begin{cases} 1, & rand(0,1) < sigmoid\left(x_i\right) \\ 0, & rand(0,1) \ge sigmoid\left(x_i\right) \end{cases} \tag{10}$$

And $sigmoid(x_i)$ is given by

$$sigmoid\left(y_i\right) = \frac{1}{1 + e^{-x_i}} \tag{11}$$

The position update is done by

$$x_i^{g+1} = x_i^g \otimes v_i^g \tag{12}$$

where, g represents the g^{th} iteration or generation. The $\otimes$ operator is defined as

$$x_i^{g+1} = \begin{cases} x_i^g, & v_i = 0 \\ N_{best_i}, & v_i = 1 \end{cases} \tag{13}$$

Therefore, the ⊗ operator ensures that the swarm is directed to a better solution. The parameter $N_{best\,i}$ is given by

$$N_{best\,i} = \arg\max_{r} \sum_{j\in N} \phi\left(x_i^g, r\right) \tag{14}$$

where $N = \{n_1, n_2, \dots, n_d\}$ is the set of neighbours to a vertex i and the function $\phi(i, j)$ is defined as

$$\phi(i, j) = \begin{cases} 1, & i = j \\ 0, & otherwise \end{cases} \tag{15}$$

$N_{best\,i}$ gives the position found among the neighbouring vertices of i^{th} vertex. Equations (12)-(15) ensure that the i^{th} vertex identifies the cluster with members similar in nature to the i^{th} vertex. The initialisation procedure involves a label propagation technique, as described by reference (36). Let the set of neighbouring vertices to vertex i be denoted as $N = \{n_1, n_2, \dots, n_d\}$, and the cluster label is denoted as $C(i)$. Initially, each vertex is assigned its own cluster label, i.e., $C(i) = i$. Subsequently, the labels are permitted to propagate throughout the network such that each vertex joins a cluster whose members exhibit similarity in properties, akin to the principles elucidated in Equations (14)-(15). Through iterative label propagation, densely connected vertices converge upon a consensus regarding an exclusive label. Consequently, with an initial population size of p, the initial positions and velocities of the particles are denoted as $X_i^1 = \{x_1^1,\ x_2^1,\ \dots,\ x_p^1\}$ and, $V_i^1 = \{v_1^1,\ v_2^1,\ \dots,\ v_p^1\}$ respectively. Moreover, the initial global best particle, G_{best} , is randomly selected from the neighbourhood set N. The discussed approach enhances diversity within the population and contributes to reduced time complexity.

Next, a turbulence operator is included to help preserve diversity within the optimization process by infusing randomness into the search trajectory. The operator's primary function is to avoid premature convergence by fostering exploration across the search space, thus enabling the identification of better solutions. This study utilises the well-established neighbour-based mutation (NBM) technique. In NBM, a random number r is generated for each vertex, such that $r \in [0, 1]$. If r is below the specified mutation probability threshold p_m , the algorithm iterates through each neighbouring vertex and assigns the vertex's label to the adjacent vertices. Consequently, the operator randomly selects a subset of the population and propagates their positions to neighbouring vertices. This operator is applied after the velocity update step of the optimization algorithm.

Finally, the Tchebycheff approach is strategically employed to decompose the multi-objective problem into a scalar problem. This method, characterised by its weighted sum approach, operates without the prerequisite of convexity assumption within the objective function. The scalar optimization problem is:

$$\min h(x|\beta, Z^*) = \max_{m\in M} \left\{ \beta_m \left| \left(f_m(x) - z_m^* \right) \right| \right\} \quad s.t.\ x \in C \tag{14a}$$

where $m \in \{1, 2, \dots, M\}$ and M is the number of objectives. $f_m()$ is the m^{th} objective function and $\beta = (\beta_1, \dots, \beta_m)$ is the weight vector. $Z^* = \{z_1^*, \dots, z_M^*\}$ is the reference vector such that $z_m^* = \{\min f_m(x)|x \in C\}$ for each $m = 1, \dots, M$. $f_m(x)$ is the value of the m^{th} objective. If for the i^{th}particle, $h(x_i^{g+1}|\beta, Z^*) < h(x_i^g|\beta, Z^*)$, then $x_i^{g+1} = x_i^g$, i.e., DPSO update the $P_{best\,i}$ otherwise $P_{best\,i}$ retains the existing value. The decisive solution from the Pareto front is identified based on the Normalised Mutual Information (NMI) index. NMI calculation takes input the categorical vertex labels, obtained from the discretisation of network optimization flow and reflects the underlying community structure of the network. The DPSO uses the *normalized_mutual_info_score* function from the *sklearn.metrics.cluster* module to calculate the NMI.

3.3. Sub-sector boundary design

The sub-sector boundaries should be connected, and shapes should exhibit compactness and convexity. This study proposes the use of a Minimum Bounding Geometry (MBG)-coupled Rule-based Approach to achieve the desired results. The design procedure is summarised below.

Input: Set of vertices V and their respective cluster labels $\{k_1,\ k_2, \dots,\ k_C\}$

Step 1: MBG
for each Cluster k_i
  construct bounding box Envelope p_i
end for

Step 2: Rule-based Approach

construct Grid with Grid centres
sort Envelopes based on increasing number of overlaps (with neighbouring Envelopes), $p^{(1)},\ p^{(2)}, \dots, p^{(C)}$
while $j \le C|p^{(j)}$ is having smallest number of overlaps
  for $i = j + 1$ *to* C do
    check for Realignment with neighbouring Envelopes $p^{(i)}$
    perform Realignment
  end for
  Modify Realigned Envelope $p^{(j)}$ to surrounding sector shapes
  j ++
end while

The check for Realignment is conducted to identify two aspects: (i) the neighbouring Envelopes, $p^{(i)},\ i = \{j+1, \dots, C\}$ overlapping with the Envelope under consideration, $p^{(j)}$, and (ii) the type of Realignment needed to be performed between the Envelope under consideration, $p^{(j)}$ and its neighbouring Envelopes, $p^{(i)},\ i = \{j+1, \dots, C\}$. This study proposes the use of two Realignment strategies, (i) Horizontal Realignment and (ii) Vertical Realignment. The fundamental procedure for both Realignment strategies are similar and is summarised below.

Horizontal Realignment
for two neighbouring Envelopes $p^{(i)}$ and $p^{(j)}$
  slide overlapping horizontal Envelope lines such that
  direction of sliding is parallel to vertical axis and away from each other
  total discrete traffic load value exchanged from $p^{(i)} \to p^{(j)} \sim$ total discrete traffic load value exchanged from $p^{(j)} \to p^{(i)}$
  sliding ends on the nearest grid line or grid center such that
    final Envelope lines are collinear
    final Envelope lines are near to route intersection points
end for
Vertical Realignment
for two neighbouring Envelopes $p^{(i)}$ and $p^{(j)}$
  slide overlapping vertical Envelope lines such that
  direction of sliding is parallel to horizontal axis and away from each other
  total discrete traffic load value exchanged from $p^{(i)} \to p^{(j)} \sim$ total discrete traffic load value exchanged from $p^{(j)} \to p^{(i)}$
  sliding ends on the nearest grid line or grid center such that
    final Envelope lines are collinear
    final Envelope lines are near to route intersection points
end for

The Horizontal and Vertical Realignment strategies, along with the Modification step, are also illustrated in Fig.s 3 and 4, respectively. The type of Realignment is selected based on the degree of overlap. For example, in Fig. 3, there are two Envelopes corresponding to the two clusters, red and blue. Horizontal Realignment leads to the possible exchange of a total of two vertices. On the contrary, Vertical Realignment will lead to the possible exchange of a total of five vertices. Hence, Horizontal Realignment is the preferred option. During the process, the overlapping Envelope lines are moved such that a vertex from the red cluster with a discrete traffic load of one goes to the blue cluster. Similarly, a vertex from the blue cluster with a discrete traffic load of one goes to the red cluster. Hence, the total traffic load exchanged between two Envelopes are balanced. The movement ends on the nearest horizontal grid line, and the earlier overlapping Envelope lines are now collinear. Lastly, the two Envelopes are modified to match the shapes of the surrounding sector, leading to two sectors. In the case of Fig. 4, there are two Envelopes corresponding to the two clusters, red and blue. Horizontal Realignment leads to the possible exchange of a total of three vertices. On the contrary, Vertical Realignment will lead to the possible exchange of only two vertices. Hence, Vertical Realignment is the preferred option. During the process, the overlapping Envelope lines are

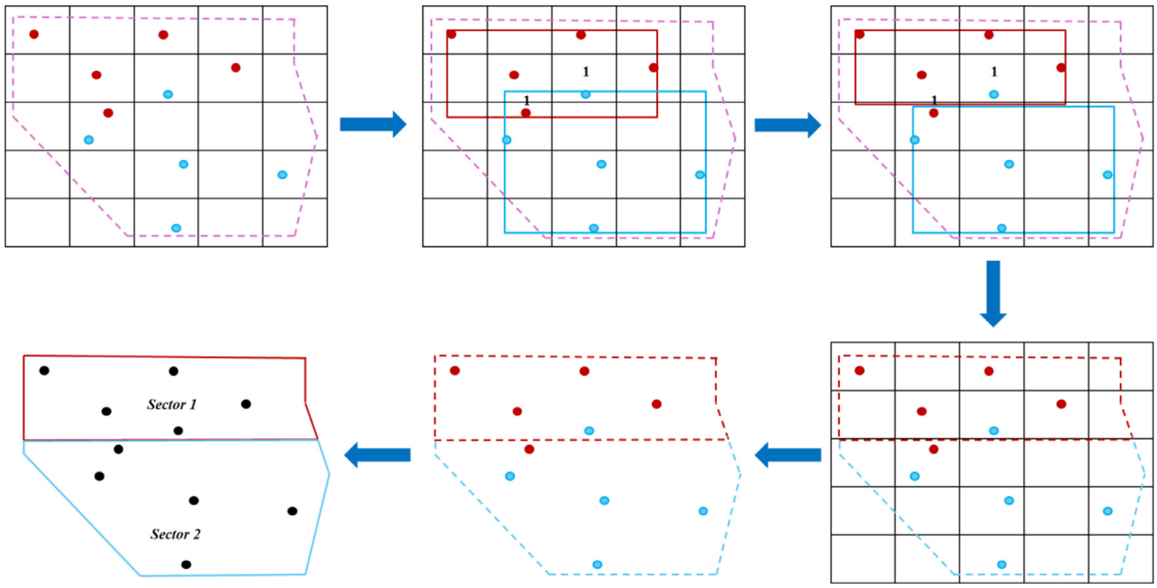

Fig. 3. Illustration of The Horizontal Realignment Followed by Modification of Envelope Boundaries.

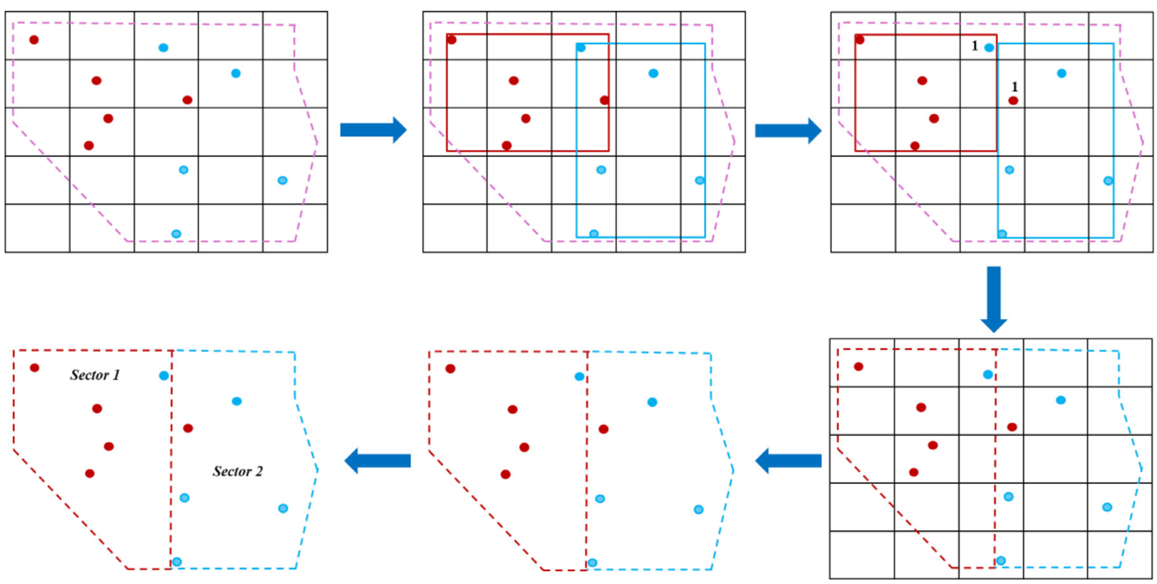

Fig. 4. Illustration of The Vertical Realignment Followed by Modification of Envelope Boundaries.

moved such that a vertex from the red cluster with a discrete traffic load of one goes to the blue cluster. Similarly, a vertex from the blue cluster with a discrete traffic load of one goes to the red cluster. Hence, the total traffic load exchanged between two Envelopes are again balanced. The movement ends on the nearest vertical grid centre and the earlier overlapping Envelope lines are now collinear. Finally, the two Envelopes are modified to match the shapes of the surrounding sector, leading to two sectors.

4. Experimental setup

This study applies the research design to Indian airspace. Despite facing a decline in traffic due to the COVID-19 pandemic, India's aviation sector has reached pre-pandemic levels by the end of 2023 and is bound to become the world's third-largest stakeholder in the world aviation market (IATA 2023; PwC 2022). Recent research underscores the complex and fluctuating patterns of air traffic in India, necessitating the advancement of infrastruture planning, monitoring strategies, and demand-capacity imbalance moderation policies in future ATM systems (Chandra et al. 2022, 2023, 2024a, 2024b). Currently, the Indian airspace comprises 18 sectors characterised by irregular shapes and uneven traffic distribution, as illustrated in Fig. 5.

Data on Indian airspace was obtained from the Airports Authority of India's open-source Aeronautical Information Services platform (Airports Authority of India, 2023,2021). Apart from India's rising inflow and outflow traffic, the existing airspace sectors also experience flyover traffic due to international flights travelling between Southeast Asia and the Middle East. Therefore, taking the case of Indian airspace sectors deems fit. Fig. 6 displays the waypoints, including navigation aids and airports, within the Indian airspace. For simplicity in implementation and discussion, we have chosen to focus on a specific sector known as VOMF-UPPER-UML (VUU) in the southwestern region, also depicted in Fig. 6. VUU is strategically positioned between the heavily Chennai and Mumbai-bound airspace sectors and constitutes significant waypoints and routes. VUU comprises 58 waypoints leading to a network of 58 vertices. The presence of significant waypoints and routes

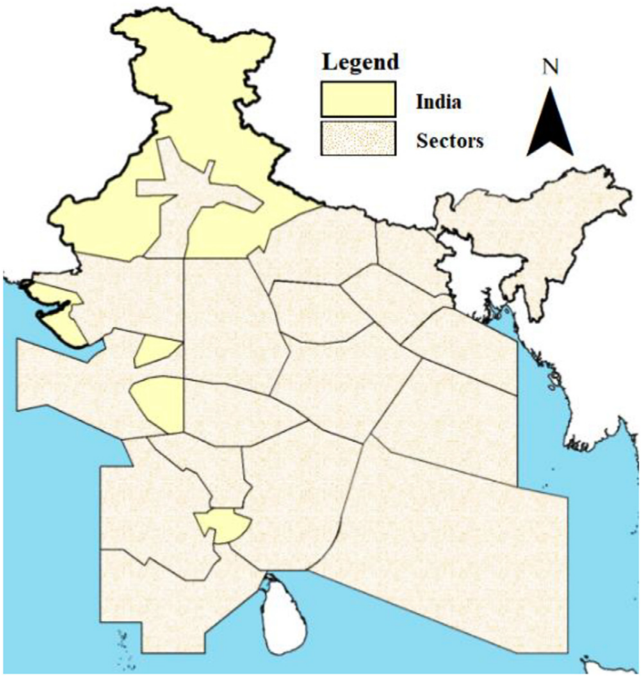

Fig. 5. Indian airspace and sectors.

in this sector results in a complex network topology, making it an ideal candidate for testing and validating the proposed research design.

The waypoints and routes within the VUU sector are represented as a directed network graph, based on the 58 × 58, 0-1 adjacency matrix. The directed graph is depicted in Fig. 7. Utilising the adjacency matrix and vertex locations, we further calculate a distance matrix using the Haversine formula. The heatmap summarising the distance matrix is illustrated in Fig. 8. Additionally, the Origin-Destination (OD) demand data is obtained from the Directorate General of Civil Aviation (DGCA) for the month of December 2022. The DGCA provides monthly passenger flow data, which is then used to derive daily passenger flow data. Subsequently, the daily passenger flow data is converted into aircraft flow data, considering an average load factor of 88.84. The OD flow of selected OD pairs is represented using a Sankey diagram in Fig. 9. In Fig. 9, the different OD pairs are represented by connecting lines, and the thickness of the lines represents the magnitude of demand. Higher line thickness represents higher demand.

The multi-commodity flow problem is addressed using the open-source Solving Constraint Integer Programs (SCIP) library. In this implementation, the edge capacity, $C_{u,v}$ is uniformly set to 50 for all edges. We employ the DPSO algorithm with a population size of 100. The cognitive and social components, denoted as s_1 and s_2, are both assigned a value of 1.494. The inertia weight, γ, and the parameters z_1 and z_2 are randomly selected from the range $[0, 1]$. Additionally, the mutation probability, p_m, is set to 0.1, and the neighbourhood size is kept at 20. These DPSO parameters are chosen based on previous recommendations. The termination criteria for the algorithm are determined by the maximum number of generations ($maxgen$) or iterations. This study conducts experiments using four different $maxgen$ values: 50, 100, 150, and 200. We implemented the DPSO in Python as well using the openly available source code. The complete experimental setup utilises a machine running the Windows 10 operating system, equipped with an AMD Ryzen 7 5800 processor operating at 3.20 GHz and 16 GB of RAM.

5. Results and discussions

The optimal incoming flow in each node is illustrated in Fig. 10. The optimal flow values ranged from 0 to 186 flights. As a result, the Low traffic load vertices will have a total incoming flow in the range [0,62]. Medium traffic load vertices will have a total incoming flow in the range of (62, 124]. Finally, High traffic load vertices will have a total incoming flow in the range of (124, 186]. The same classification is reflected in the categorical traffic load assignment, also shown in Fig. 10. It is worth noting that only four vertices exhibit high traffic load: Mangalore, Goa, Calicut, and Coimbatore airports. All four are international airports with significant international and domestic traffic.

Among the medium traffic load vertices, all are waypoints except one airport, the Kochi International Airport. Low traffic load vertices are

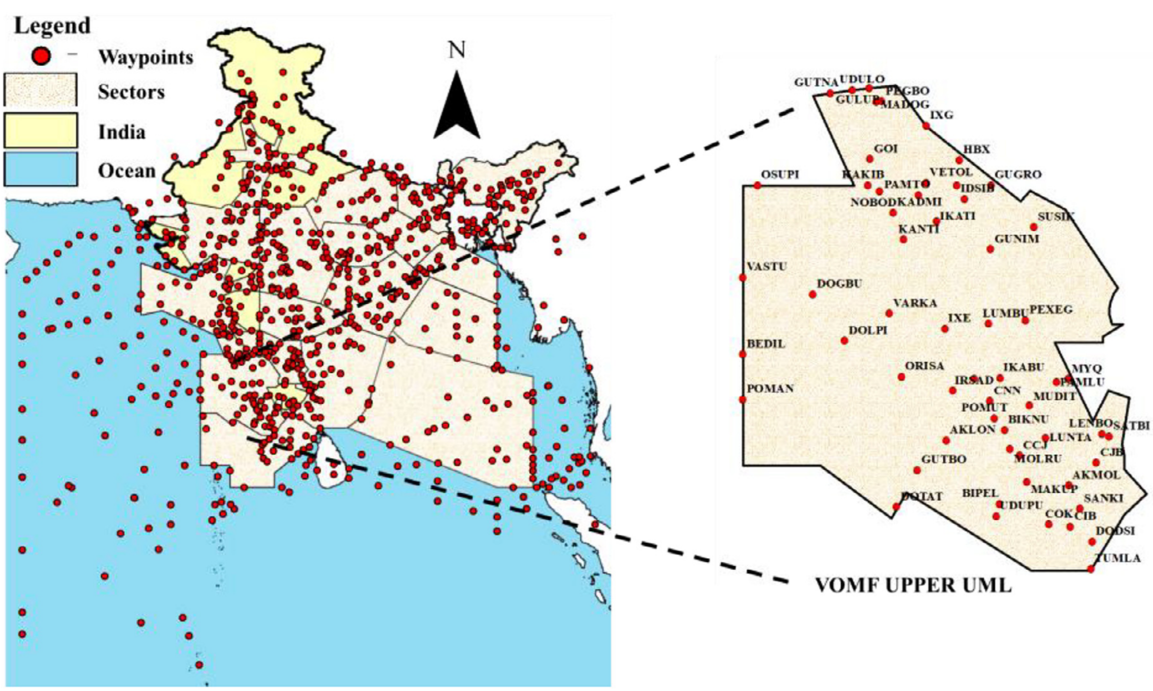

Fig. 6. Sector selected for implementing the proposed methodology.

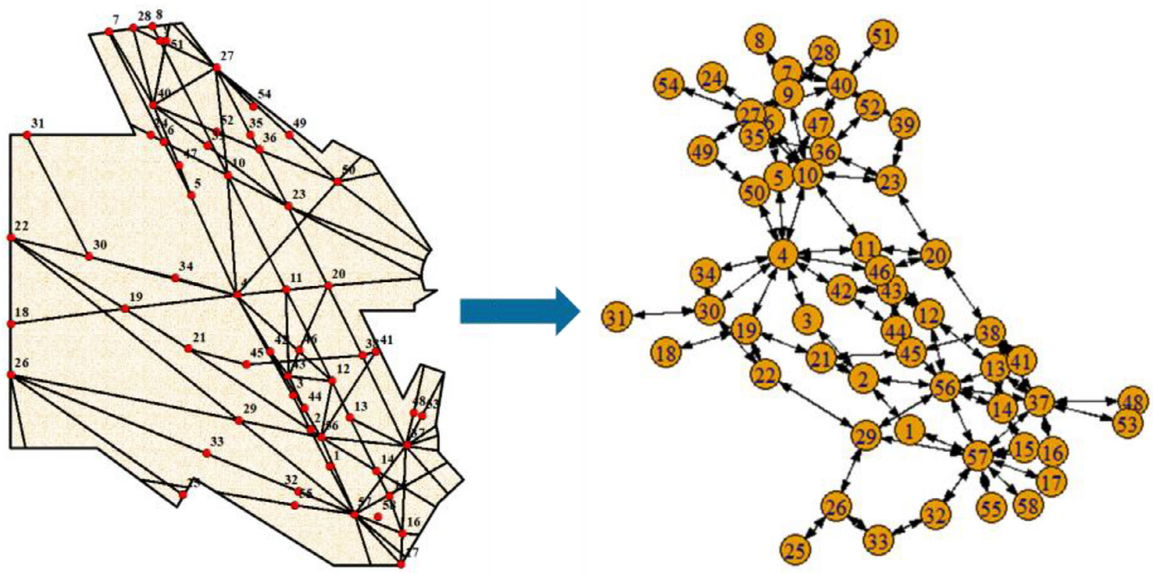

Fig. 7. Network graph created based on the waypoints and routes in VUU Sector.

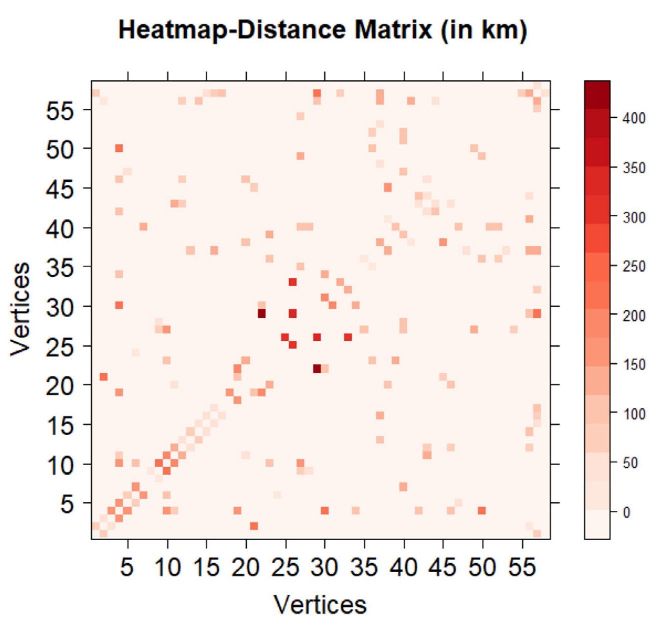

Fig. 8. Heat map of the distance matrix (in km).

Table 2
Variation of cluster number and cluster size with ***maxgen***.

	Number of Vertices				
	maxgen →	50	100	150	200
Clusters ↓	**C0**	20	28	21	10
	C1	11	16	20	20
	C2	04	14	12	28
	C3	13	–	05	–
	C4	10	–	–	–
	Total	**58**	**58**	**58**	**58**

Table 3
Variation of average traffic load within a Cluster with ***maxgen***.

	Average Traffic Load				
	maxgen →	50	100	150	200
Clusters ↓	**C0**	1.15	1.25	1.62	1.40
	C1	1.64	1.56	1.15	1.30
	C2	1.00	1.21	1.10	1.32
	C3	1.38	–	1.40	–
	C4	1.40	–	–	–

gained mostly from waypoints or smaller airports with limited domestic connectivity. Therefore, the optimal flow values from MCFP reflect the real operational scenario of the VUU sector. The clustering algorithm is implemented considering the categorical load as input. Clustering results put forward several interesting observations. The first set of observations consists of the fluctuation in cluster size with varying *maxgen* values, as outlined in Table 2. When *maxgen* is set as 50, the DPSO identifies five clusters. These clusters are labelled as C0, C1, C2, C3, and C4 in Table 2. The four clusters, respectively, have 20, 11, 4, 13, and 10 vertices. Increasing *maxgen* to 100 results in three clusters: C0, C1, and C2, with 28, 16, and 14 vertices, respectively. At $maxgen = 150$, the DPSO detects four clusters, C0, C1, C2, and C3. The respective cluster sizes are 21, 20, 12, and 5 vertices. Finally, setting $maxgen = 200$ identifies three clusters with sizes 10, 20, and 28 vertices. Evidently, the clustering outcomes vary in response to changes in the number of generations or iterations. Further, the clusters associated with $maxgen = 50$ exhibit a more uniform cluster size distribution followed by results associated with $maxgen = 150$ and $maxgen = 100$. In essence, the distribution of vertices across different clusters is more balanced.

Similar trends emerge when examining the average traffic load variation among clusters for different *maxgen* values. Table 3 reports the variation in average traffic load within clusters for varying *maxgen* values. When *maxgen* is set as 50, the resulting clusters C0, C1, C2, C3, and C4 exhibit average traffic loads of 1.15, 1.64, 1.00, 1.38, and 1.40, respectively. The three clusters C0, C1, and C2 corresponding to $maxgen = 100$ have average traffic loads of 1.25, 1.56, and 1.21, respectively. When *maxgen* is set as 150, the resulting clusters C0, C1, C2, and C3 exhibit average traffic loads of 1.62, 1.15, 1.10, and 1.40, respectively. Finally, at $maxgen = 200$, the three clusters, C0, C1, and C2, have average traffic loads of 1.40, 1.30, and 1.32, respectively. Observations from Table 3 suggest that the proposed method can generate clusters with more balanced average traffic loads. However, traffic load distribution among clusters varies across different *maxgen* values.

Contrary to the observations in Table 2, the findings associated with $maxgen = 200$ indicate the best equitable distribution of traffic load

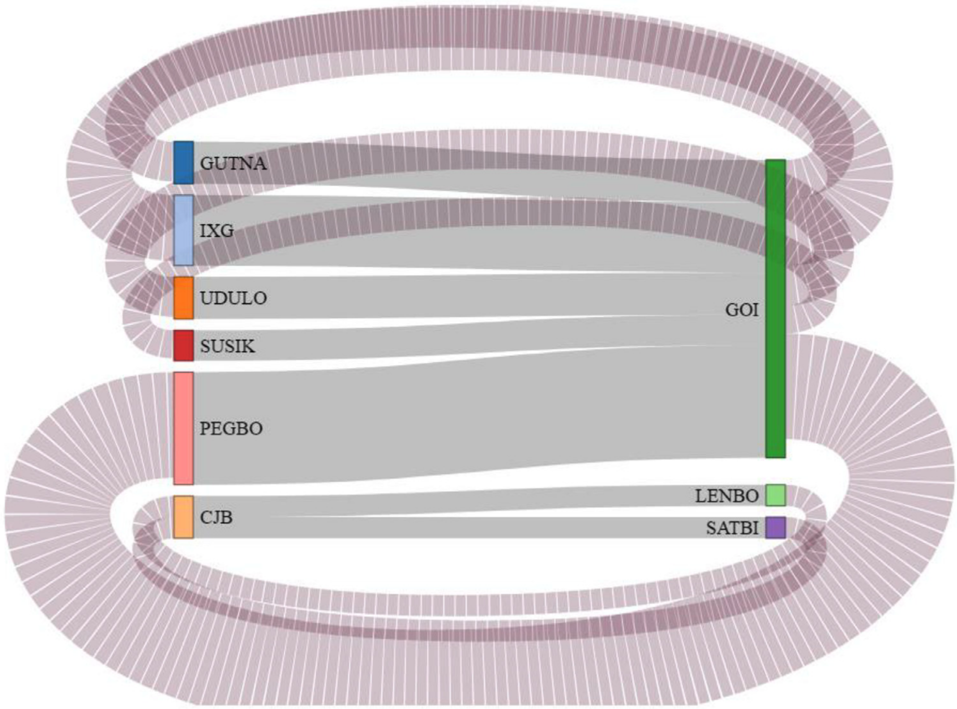

Fig. 9. Sankey diagram representing Deman between selected OD Pairs.

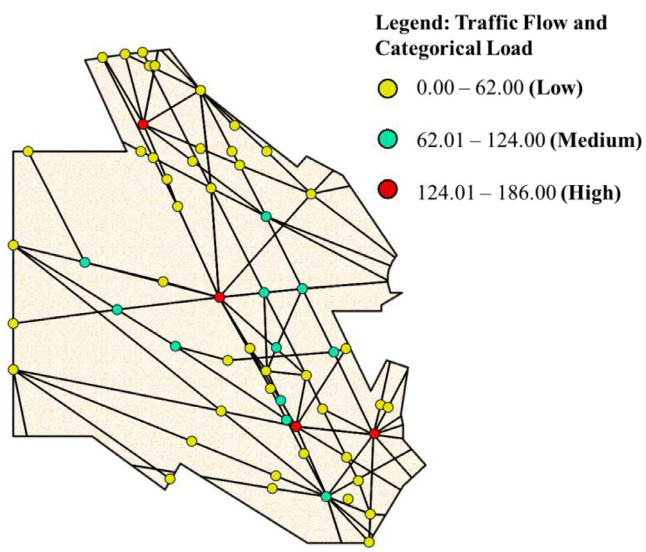

Fig. 10. Traffic flow output from solving MCFP and corresponding categorical traffic load.

among clusters. The next degree of traffic load distribution is then visible in results corresponding to *maxgen* = 100 and *maxgen* = 150. These overall observations align with the network clustering literature, where Gong et al. (Gong & Ma et al. 2012) proposed that the MODPSO algorithm performs at *maxgen* = 140. Given the array of results, we performed further analysis to identify the best case. The set feasible solutions at each *maxgen* value is shown in Fig. 11. At *maxgen* = 50, DPSO yields 51 feasible solutions. At *maxgen* = 100, DPSO yields eight solutions. The number of feasible solutions at *maxgen* = 150 and *maxgen* = 200 are 55 and 37, respectively. Fig. 12 illustrates the variation of the minimum value of the objective functions among all the feasible solutions in each generation for different *maxgen* cases.

When *maxgen* is set as 50, the minimum of LDWC among the set of feasible solutions decreases with generations and attains the lowest value at the 30th generation, followed by an increase from 38th generation. Similarly, the minimum of LDBC among the set of feasible solutions decreases with generations. However, the minimum LDBC among the set of feasible solutions attains the lowest value at the 23rd generation but increases at the 40th generation. When *maxgen* is set as 100, the minimum of LDWC and LDBC among the set of feasible solutions does not exhibit much variation with generations. The minimum of LDWC attains the lowest value for the 9th generation and remains stable. The minimum LDBC among the set of feasible solutions attains the lowest value at the 8th generation and remains stable. In the case of 150 generations, the minimum of LDWC among the set of feasible solutions gain decreases with generations and attains the lowest value at the 75th generation with slight fluctuations in subsequent generations but again stabilises from the 145th generation. The minimum LDBC attains the lowest value at the 36th generation and remains stable. In the case of 200 generations, the minimum LDWC among the set of feasible solutions attains the lowest value at the 36th generation and then remains stable. The minimum LDBC among the set of feasible solutions attains the lowest value at the 11th generation and remains consistent for subsequent generations.

The combined interpretations from Fig.s 11 and 12 suggest that DPSO results corresponding to *maxgen* = 150 perform comparatively better for LDWC objective. Simultaneously, the DPSO results corresponding to *maxgen* = 100 and 200 perform comparatively better for the LDBC objective. Among both cases, results corresponding to *maxgen* = 100 perform better for the LDWC objective. To gain further insights, the variation of modularity values (Q) among the population is examined at different *maxgen* values. Corresponding results are depicted in Fig. 13. Modularity serves as an indicator of community strength within a network, with higher values indicating denser communities. The cases with *maxgen* = 100 and *maxgen* = 200 are very similar in terms of modularity results. The case with *maxgen* = 100 exhibits the maximum and average modularity values of 0.471 and 0.468, respectively. For the case of *maxgen* = 200, the maximum and average modularity values are 0.482 and 0.424, respectively. Similarly, the cases with *maxgen* = 50 and *maxgen* = 150 are comparable. The case with *maxgen* = 50 exhibits the maximum and average modularity values of 0.553 and 0.536, respectively. In the case of *maxgen* = 150, modularity values are slightly higher, with maximum and average values of 0.561 and 0.532, respectively.

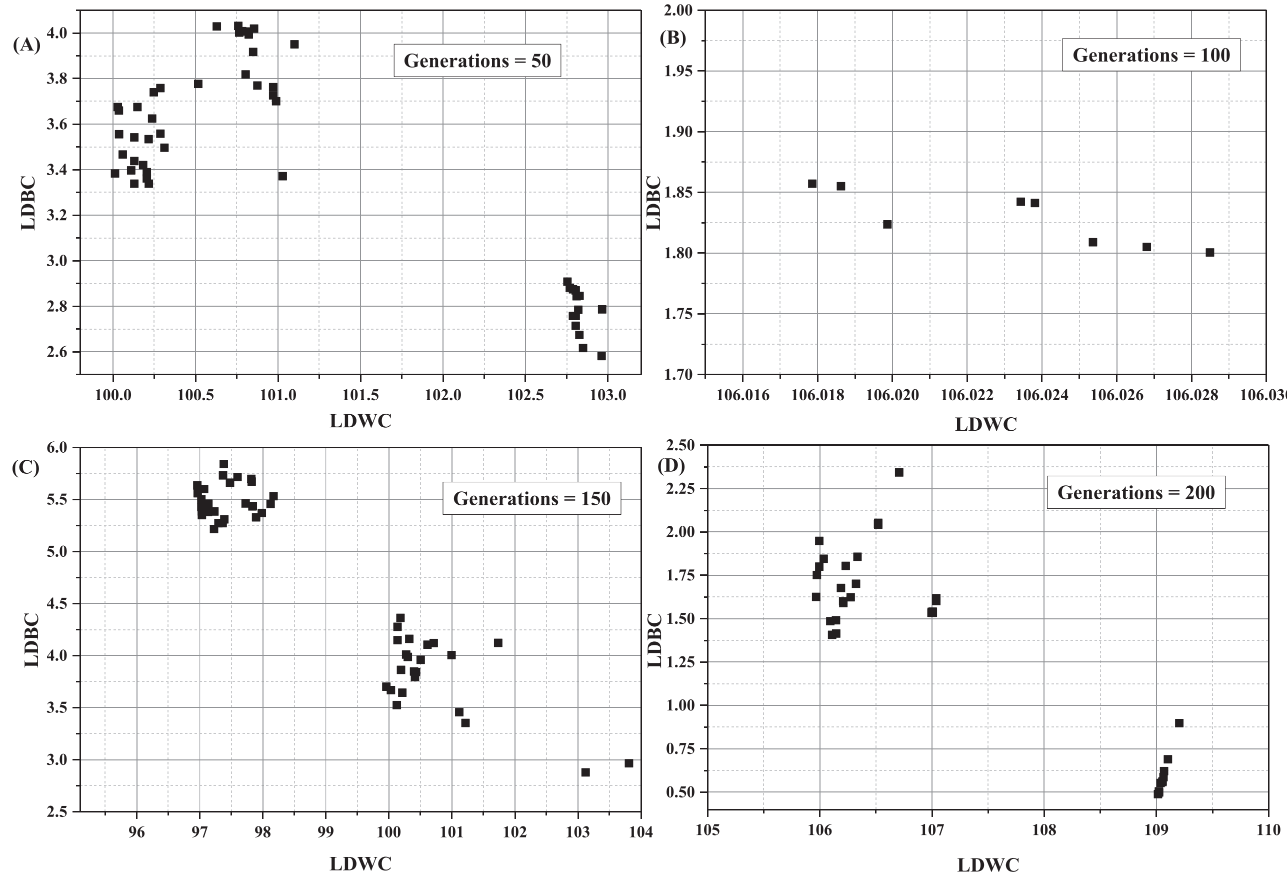

Fig. 11. Set of Feasible Solutions at Different ***maxgen*** Values (11A: ***maxgen***=50, 11B: ***maxgen***=100, 11C: ***maxgen***=150, 11D: ***maxgen***=200.

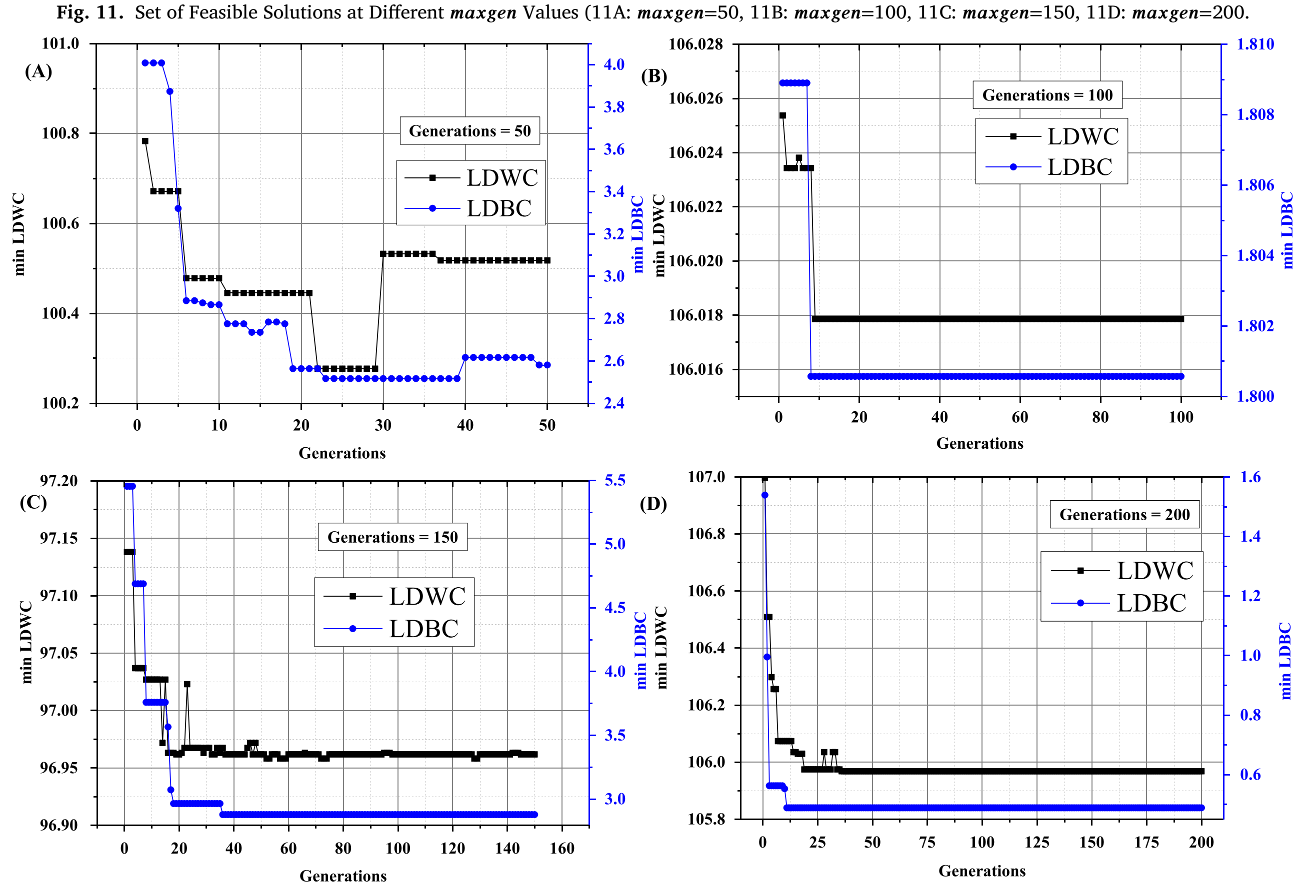

Fig. 12. Variation of Minimum Values of Objective Function for Different ***maxgen*** Values (12A: ***maxgen*** = 50, 12B: ***maxgen*** = 100, 12C: ***maxgen*** = 150, 12D: ***maxgen*** = 200).

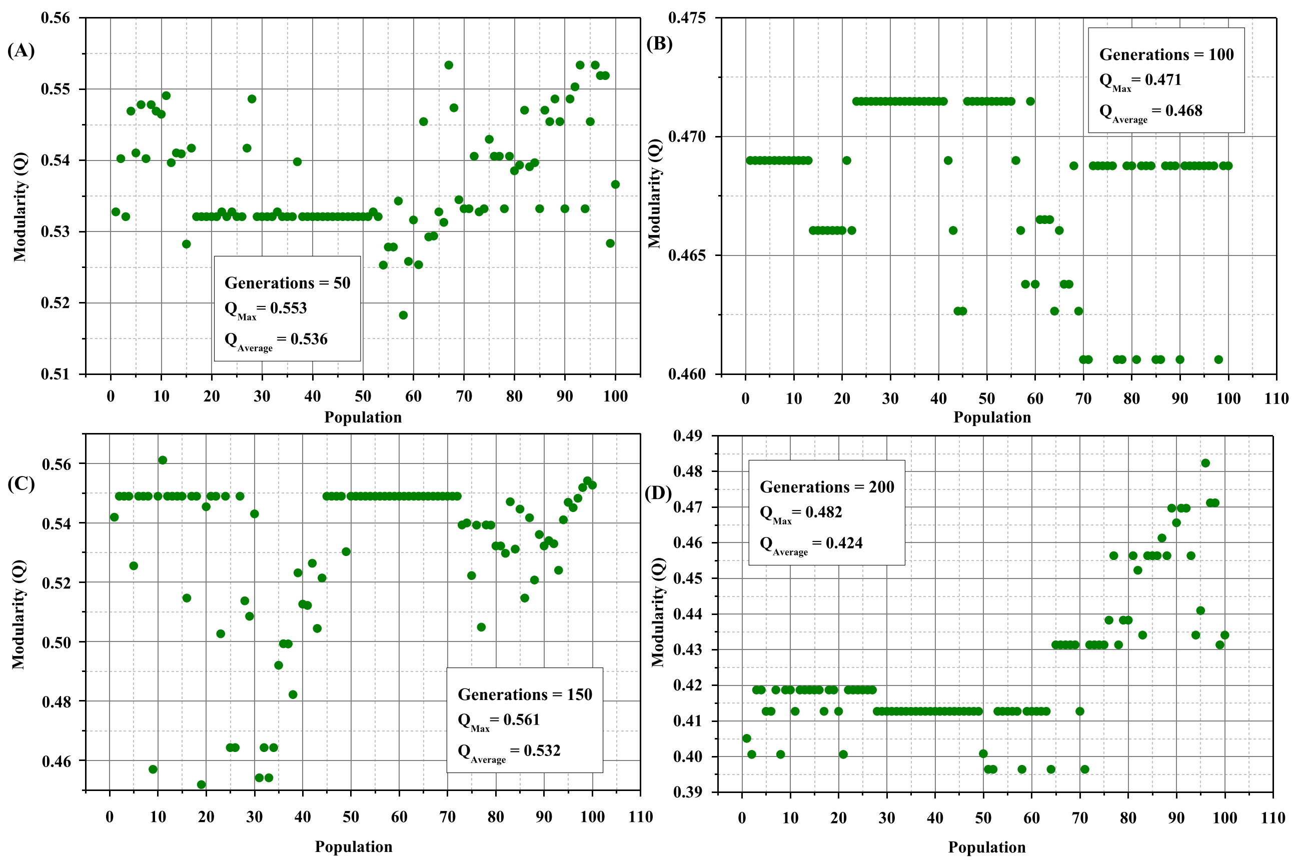

Fig. 13. Variation of Modularity within the Swarm Population with ***maxgen*** Values (13A: ***maxgen*** = 50, 13B: ***maxgen*** = 100, 13C: ***maxgen*** = 150, 13D: ***maxgen*** = 200).

The cluster output corresponding to four *maxgen* cases are summarised in Fig. 14. It is evident that cluster results for *maxgen* = 50 and *maxgen* = 150 are almost similar, hence similar modularity values. Considering the comprehensive observations on optimality, modularity, balanced traffic load, and uniform cluster size, this study selects the cluster output corresponding to *maxgen* = 100 and *maxgen* = 150 for sub-sector boundary design. The boundary design for *maxgen* = 100 case is given in Fig. 15. Boundary design for *maxgen* = 150 case is given in Fig. 16. Figs 15 and 16 also provide the MBG-based envelope design, grid layout, envelope boundary realignment, and final sub-sector boundaries. Fig. 15A indicates the three convex Envelopes because of the MBG method. Once the grid is created, we look for the Realignment of the Envelope. Envelope 1 has only one overlap with Envelope 2. Therefore, the approach starts with Envelope 1. Envelope 1 and Envelope 2 will undergo envelope realignment. Here, horizontal Realignment will take place as it leads to the least number of vertex exchanges. The horizontal Realignment takes place such that Envelope 1 gains two vertices from Envelope 2 with a total discrete value of 4. Subsequently, it loses three vertices to Envelope 2 with a total discrete value of 4. The next Envelope with the least overlap is Envelope 3, which overlaps with Envelope 2. Hence, the approach proceeds for the Realignment with Envelope 3. Again, only horizontal Realignment takes place. The Realignment happens such that Envelope 2 gains three vertices from Envelope 3 with a total discrete value of 3. Simultaneously, Envelope 2 loses two vertices to Envelope 3 with a total discrete value of 4. The next turn is for Envelope 2, but all the Realignment for this Envelope are already achieved. Final realigned Envelopes are given in Fig. 15C, followed by final sub-sector boundaries in Fig. 15D. After the rule-based approach, the average traffic load in Sub-Sector 1, 2, and 3 are 1.30, 1.33, and 1.38, respectively. Respective cluster sizes are 27, 18, and 13.

Fig. 16A indicates the four convex envelopes as a result of the MBG method. Once the grid is created, we look for Realignment of the Envelope. Envelope 2 has only one overlap with Envelope 1. Therefore, Envelope 2 and Envelope 1 will undergo Envelope Realignment. Here, only vertical Realignment is takes place due to the least requirement of vertex exchange. The vertical Realignment takes place such that no Envelope gains or loses any vertex. Next Envelope with the least degree of overlap is Envelope 4, which shares boundaries with Envelope 3. A vertical realignment takes place between Envelopes 4 and 3, where two vertices are exchanged among them, each of low traffic load. The total discrete value gained and lost is 2. The next Envelope with the least overlaps is Envelope 3. After its Realignment with Envelope 4, it only overlaps with Envelope 1. As per the approach, it performs a horizontal realignment with Envelope 1. The Realignment happens such that Envelope 4 gains one vertex from Envelope 1 with a total discrete value of 3. Simultaneously, Envelope 4 loses three vertices to Envelope 1 with a total discrete value of 3. The next turn is for Envelope 1 but all Realignment for this Envelope has already been achieved. Final realigned envelopes are given in Fig. 16C followed by final sub-sector boundaries in Fig. 16D. After the rule-based approach, the average traffic load in sub-sectors 1, 2, 3, and 4 are 1.47, 1.15, 1.30, 1.40, respectively. Respective cluster sizes are 27, 18, and 13. Respective cluster sizes are 23, 20, and 10, and 5. It is worth noting that a lesser number of clusters leads to a smoother application of the Rule-based approach. Nevertheless, the Rule-based approach continues to ensure that all sub-sectors are equitable and balanced. Overall observations indicate the applicability of the proposed research on obtaining desirable airspace sub-sectors, thus contributing to efficient air traffic monitoring, reducing controller workload, and minimising safety concerns. The overall results and inferences are promising and have interesting implications. The subsequent sec-

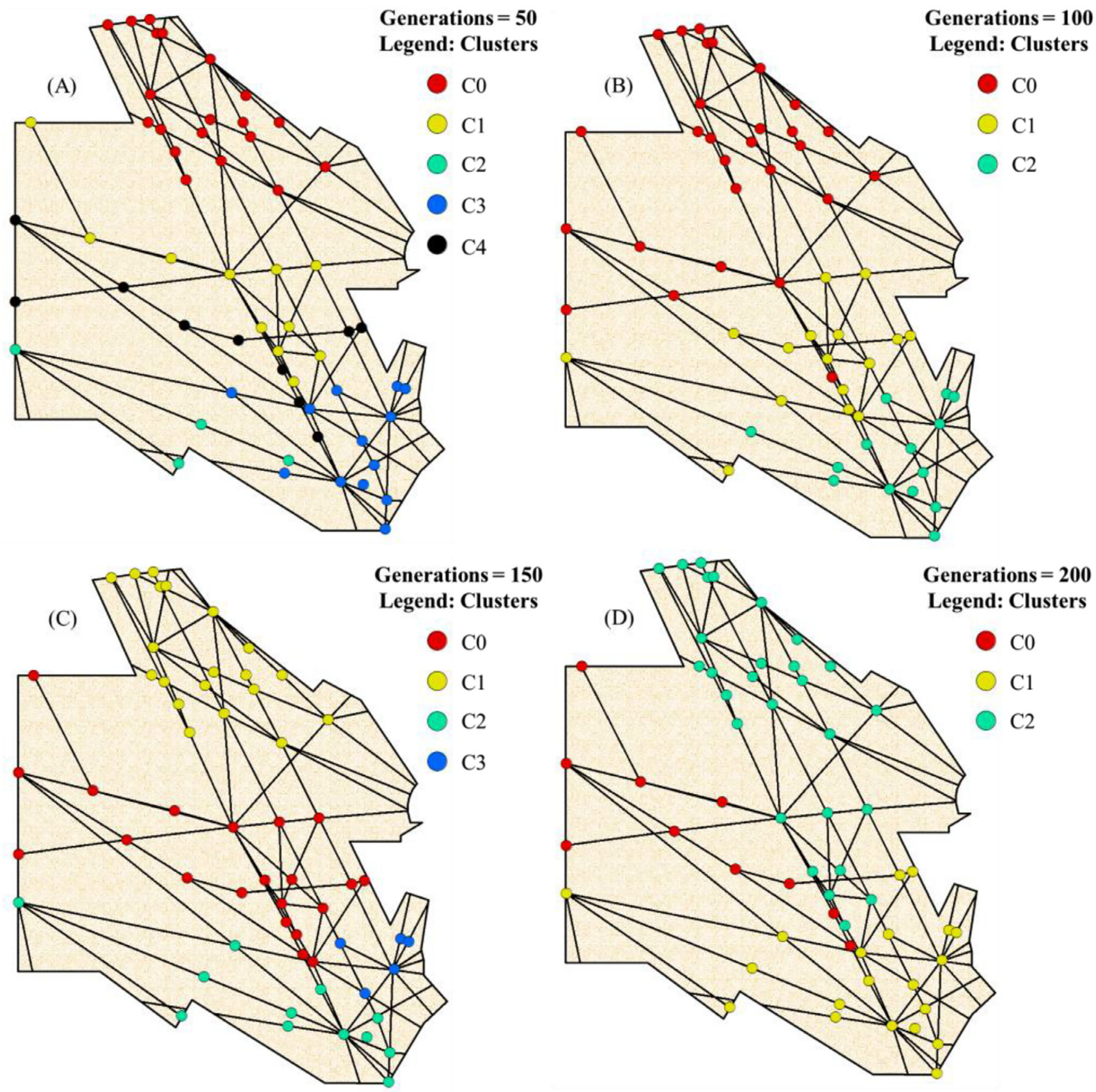

Fig. 14. Clustering Results for Different $\boldsymbol{maxgen}$ Values (14A: $\boldsymbol{maxgen} = 50$, 14B: $\boldsymbol{maxgen} = 100$, 14C: $\boldsymbol{maxgen} = 150$, 14D: $\boldsymbol{maxgen} = 200$).

tion discusses the implications, limitations, and research opportunities arising from the present study.

6. Research implications and limitations

The research findings offer several implications for the advancement of airspace sectorization and air traffic management strategies. First, the network optimization formulation is crucial to obtain an orderly and regular representation of the travel demand on the network in the form of optimal flow assignment. The multi-commodity flow model possesses sufficient static-to-dynamic and dynamic-to-static adaptability to represent the dynamic demand conditions and traffic patterns on the network. Secondly, the network clustering approach considers the inherent complex nature of air transportation networks in its formulation, contributing to a higher retention of network behaviour. Ensuring compliance with such measures improves the robustness of sectors/sub-sectors to network evolution and dynamics. The network clustering approach also has the flexibility of circumventing the need to encode connectivity, convexity, and compactness as strict constraints. Consequently, the nontrivial constrained multi-objective problem transforms into a more computationally tractable unconstrained multi-objective problem. Finally, the Minimum Bounding Geometry (MBG)-coupled Rule-based approach allows enough control over boundary design while ensuring compactness and convexity conditions. Controllability is often a desired criterion for higher acceptability among practitioners involved in en route sector design and control. Higher acceptability among practitioners fosters the development of adaptive and responsive ATM systems.

It should be noted that there can be challenges in generalizing the cluster results corresponding to 100 and 150 generations for different airspace environments and traffic patterns. However, there exists no universal rule to determine the best number of generations. Studies inspiring the present methodology have expressed suitable results at varying $maxgen$ values such as 50, 80, 100, 120, 140, and 160 (Gong & Cai et al. 2012; Gong et al., 2014). Purely from a scalability point of view, it is better to limit the highest $maxgen$ value for testing to 150. But identifying the factors affecting the best $maxgen$ value is in itself an intriguing problem statement. In essence, choosing the best $maxgen \in [50, 150]$ is a possible limitation, worthy of further investigation. Nonetheless, for the generalizability of this study, we propose a simple solution-driven framework to identify the best $maxgen$ value. First, considering the computational complexity, scalability, and recommendations from literature (Gong & Cai et al. 2012; Gong et al., 2014),

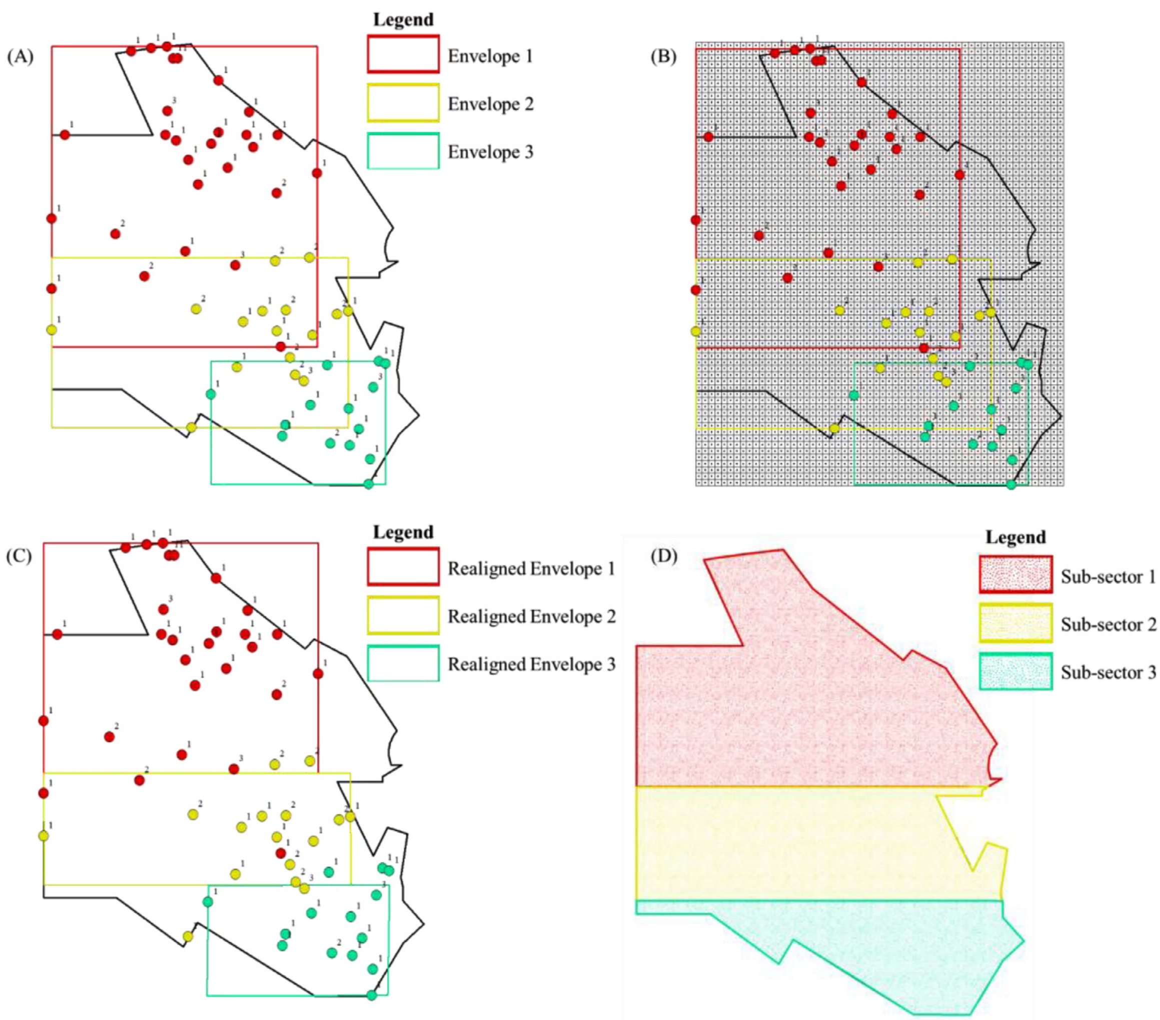

Fig. 15. Sub-sector Boundary Design for Clustering Results Corresponding to $\boldsymbol{maxgen} = 100$ (15A: MBG-based envelope design, 15B: Grid layout, 15C: Envelope boundary realignment, 15D: Final sub-sectors **boundaries**).

it is best to keep the candidate set of $maxgen$ values $\in [50, 150]$ to run the framework. Any future study utilizing the proposed framework can generate results for the following candidate set of $maxgen$ values: 50, 80, 100, 120, 150. Once the results are generated for the candidates, the best $maxgen$ candidate can be selected based on four metrics: (i) standard deviation of cluster size, (ii) standard deviation of average cluster traffic load, (iii) values of LDWC and LDBC, and (iv) average and maximum modularity. Ideally, the best $maxgen$ candidate should produce clusters with lowest values for the first three metrics (indicating equity and stability) and highest value for the fourth metric (indicating strong community structure). In the absence of clear identification from all four metrics, the candidate having best values for the first two metrics can be considered.

Another minor but significant aspect of the integrated framework is the requirement of discretised categorical traffic load values for each vertex as guiding standards for the DPSO. Although the discretised categorical traffic load values have been obtained from the network optimization results, future work can look towards more intelligent setups. Notably, time-series based techniques like ensemble ARIMA (E-ARIMA) (Shahriari et al., 2020) and Shapelet Transform Classifier (AlDhanhani et al., 2019), etc., can be applied over long-term observed flow data to obtain more representative load classifications. Such load classifications will represent long-term traffic flow patterns over a network and may lead to more representative sectors. Therefore, the utility of discretised categorical traffic load values induces promising research directions, bypassing the need for network optimization models. An additional interesting implication arises from using the complex network clustering approach. There exists a strong association between the existence of network communities and the robustness of a transportation network (Sun and Wandelt, 2021; Wandelt et al., 2021). Literature hints towards the role of inter-community connections as networks with weak inter-community connections have been found to be more susceptible to attacks (Requião da Cunha et al., 2015). The present study aims to achieve an equitable distribution of intra-community (intracluster) and inter-community (inter-cluster) edges through the two objectives. Simultaneously, we are also taking into consideration the aspects of cluster size, modularity, equity, stability and traffic load to determine the best results. In essence, the overall framework ensures the preservation of the characteristics required for higher robustness while utilising the underlying community structures to design sectors.

These are interesting implications and research avenues, but the present study has its limitations. Presently, the paper only addresses the 2D static problem, leaving scope to address the 3D dynamic problem within an integrated framework. Translating the present framework to solve the 3D problem may require overcoming a few critical challenges. Considering 3D airspace as a set of 3D building blocks resembling a convex polytope, the first step may involve building a 3D graph. This 3D graph is expected to represent a network of building blocks. Each vertex corresponds to the centre of a block, and links connect vertices to indicate relationships between blocks. Vertices and links can be assigned weights. Vertex weights reflect the complexity of their corresponding blocks, while link weights represent the traffic flow between connected

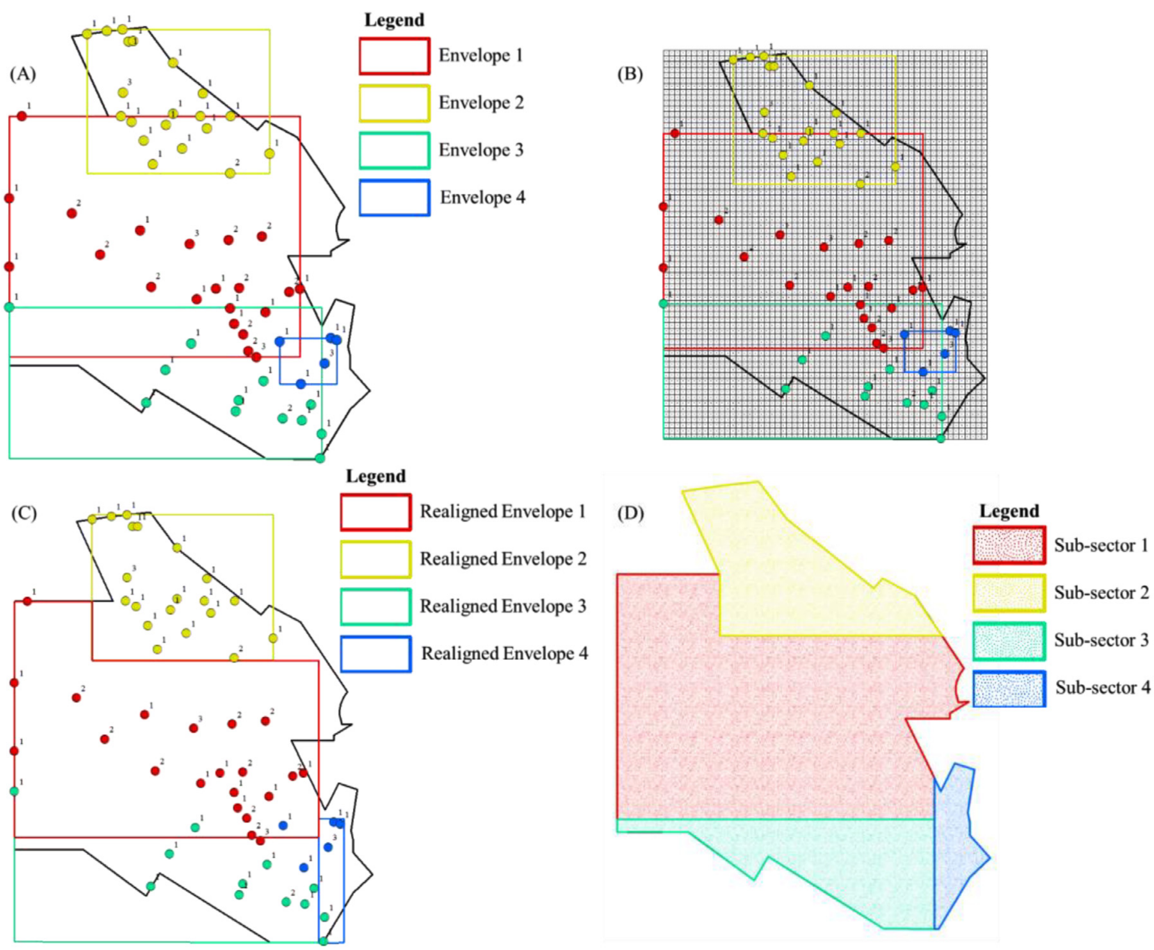

Fig. 16. Sub-sector Boundary Design for Clustering Results Corresponding to $\boldsymbol{maxgen}$ = 150 (16A: MBG-based envelope design, 16B: Grid layout, 16C: Envelope boundary realignment, 16D: Final sub-sectors boundaries).

blocks (Kim et al. 2021; Sergeeva et al. 2015). Subsequent steps may involve translating the 2D network clustering model to a 3D network clustering model built on similar theoretical foundations. Network clustering problem in 3D is an emerging and interdisciplinary field with its own set of challenges. Limited studies that explored the concept of a 3D network clustering model highlighted critical challenges such as building a regular network, higher computational complexity, and overlapping clusters (Azri et al., 2019; Fan et al. 2020; Papadakis et al., 2013). The dynamic and three-dimensional adaptability of the MBG-coupled Rule-based Approach is also another challenge and requires further introspection. The performance of the framework in rapidly changing conditions or extreme scenarios is an interesting avenue. Unfortunately, the lack of such data on our end limited the testing and validation tasks. Nevertheless, these are promising opportunities for future studies inspired by the outcomes of the present research.

7. Summary and Conclusions

This study proposes the possibility of 2D en route airspace subsectorization through a novel integrated framework. The first component of the framework involves a multi-commodity flow problem (MCFP) to find the system-wide flow assignment on the network. The input to the optimization model includes a 2D airspace directed graph with vertices and edges, edge capacity, and demand between different OD pairs where each OD demand is treated as a commodity characterised by a source, sink and demand value. Then, the flow on a vertex is calculated by summing the optimal flows from all incoming edges connected to that vertex. The second component of the framework involves a complex network clustering problem guided by the discretised category traffic load values on each vertex. A categorical weighting scheme is introduced to obtain the discrete values and respective categories. This scheme orders vertices into three categories: Low load, Medium load, and High load. Vertices with incoming flow falling within the first tertile are designated as Low load vertices, assigned a discrete traffic load value of 1. Those within the second tertile are classified as Medium load vertices, with a value of 2, while vertices in the third tertile are labelled High load vertices, assigned a value of 3. The network clustering problem is posed as an unconstrained multi-objective problem with two objectives: minimising intracluster (intra sub-sector) edge densities across different (clusters) sub-sectors and minimising intercluster (inter sub-sector) edge densities across different (clusters) sub-sectors. The clustering problem is then solved using a decomposition-based discrete particle swarm optimization (DPSO), with the decisive solution chosen based on the underlying community structure of the network represented through the categorical vertex labels. Finally, a Minimum Bounding Geometry (MBG)-coupled Rule-based Approach is proposed to design convex and compact sub-sector boundaries across the vertex clusters.

A southwester sector from Indian airspace, VOMF-UPPER-UML (VUU), comprising a network of 58 vertices and 188 directed edges, was used to experimentally validate the integrated framework. The OD pairs and demand values were obtained for December 2022 from the Directorate General of Civil Aviation (DGCA) website. The DPSO were run for four different iterations ($maxgen$), 50, 100, 150, and 200. The flow values obtained from MCFP reflect real operational conditions with large international airports exhibiting High traffic load. The clustering results indicate that cluster size varies across $maxgen$ values. The average traffic load across clusters now converge to Medium traffic load, representing a more balanced traffic load distribution. However, the degree of balance also varies across different generations. Further introspection on the objective function values, modularity, cluster size, and traffic load distribution, results corresponding to $maxgen = 100$ and $maxgen = 150$ performs better and is selected for boundary design. The MBG-coupled Rule-based Approach ensured compact and convex boundary design while ensuring that all sub-sectors remain equitable and balanced.

The primary conclusion hints towards the suitability of the integrated framework in designing equitable and balanced airspace sub-sectors. There exist a few critical implications and future research possibilities as well. The MCFP can be adapted from static to dynamic conditions, effectively capturing dynamic demand variations and traffic patterns. Therefore, the proposed framework can be adapted for dynamic sectorization problems. In addition, the network clustering approach accounts for the inherent complexity of air transportation networks, enhancing the robustness of sectors/sub-sectors to network evolution. The clustering problem bypasses the need for strict constraints on connectivity, convexity, and compactness, thus leading to a more computationally tractable unconstrained multi-objective problem. The MBG-coupled Rule-based Approach provides control over boundary design, ensuring compactness and convexity conditions, which is crucial for gaining acceptance among practitioners involved in en route sector design and control. Future research could explore more intelligent setups to determine the categorical weights to vertices with weights representative of long-term traffic flow patterns. The study's limitations include its focus on the 2D static problem, leaving room to address the more complex 3D dynamic problem using the integrated framework. The performance of the framework under rapidly changing conditions or extreme scenarios is yet to be explored. Addressing the dynamic adaptability of the MBG-coupled Rule-based Approach is another pertinent area for future research, offering promising opportunities. Future efforts are also required to test the applicability of the proposed framework to an even larger and more complex airspace system.

Declaration of competing interest

The authors declare that they have no known competing financial interests or personal relationships that could have appeared to influence the work reported in this paper.

CRediT authorship contribution statement

Aitichya Chandra: Writing – review & editing, Writing – original draft, Visualization, Validation, Methodology, Investigation, Formal analysis, Data curation, Conceptualization. **Sayan Hazra:** Writing – review & editing, Visualization, Validation, Formal analysis, Data curation. **Ashish Verma:** Writing – review & editing, Supervision, Resources, Project administration, Methodology, Funding acquisition, Conceptualization.

Acknowledgement

The authors thank PMRF PM/MHRD-20-16823.03 for the financial support and Mr. KP Sooraj, airports Authority of India, for helping us in finding the resources and data sources used in the experimental setup.

References

Airports Authority of India. 2018. *Strategic Plan for Air Navigation Services*. https://www.aai.aero/hi/system/files/resources/ANS-ST-PLAN-Version1_0-Final-December14.pdf.

Airports Authority of India. 2021. “Integrated aeronautical information package.” https://aim-india.aai.aero/eaip/PUB/2012-04-01/html/index-en-GB.html.

Airports Authority of India. 2023. “Aeronautical information services- India.” https://aim-india.aai.aero/eaip/.

AlDhanhani, Ahmed, Damiani, Ernesto, Mizouni, Rabeb, & Wang, Di (2019). Framework for traffic event detection using shapelet transform. *Engineering Applications of Artificial Intelligence, 82*(June), 226–235. 10.1016/j.engappai.2019.04.002.

Azri, S, Ujang, U, & Abdul Rahman, A (2019). 3D Geo-Clustering for Wirless Sensor Network in Smart City. 5th International Conference on Geoinformation Science – GeoAd*vances, 10-11 October 2018*: XLII.

Bagler, Ganesh. (2008). Analysis of the airport network of india as a complex weighted network. *Physica A: Statistical Mechanics and Its Applications, 387*(12), 2972–2980. 10.1016/j.physa.2008.01.077.

Bianco, Lucio, & Bielli, Maurizio (1992). Air Traffic Management: Optimization Models and Algorithms. *Journal of Advanced Transportation, 26*(2), 131–167. 10.1002/atr.5670260205.

Brinton, Chris R., & Pledgie, Stephen (2008). Airspace partitioning using flight clustering and computational geometry. *2008 IEEE/AIAA 27th Digital Avionics Systems Conference* 3.B.3-1-3.B.3-10. IEEE. 10.1109/DASC.2008.4702800.

Cai, Kai-quan, Jun Zhang, Ming-ming Xiao, Ke Tang, and Wen-bo Du. 2017. “Simultaneous optimization of airspace congestion and flight delay in air traffic network,” 1–11.

Chandra, A., Hazra, S., Verma, A., & Sooraj, K. P. (2024). On the Possibilities of Efficient Air Traffic Monitoring through Complex Network Clustering Based Airspace Sub-Sectorization: A Multi-Objective Discrete Particle Swarm Optimization Approach. *Transportation Research Record, 0*(0). https://doi.org/10.1177/03611981241263829.

Chandra, Aitichya, Choubey, Nipun, Verma, Ashish, & Sooraj, K. P. (2024a). Quasi-stochastic optimization model for time-based arrival scheduling considering standard terminal arrival (STAR) track time and a new delay-conflict relationship. *Journal of Air Transport Management, 115*(March), Article 102527. 10.1016/j.jairtraman.2023.102527.

Chandra, Aitichya, Choubey, Nipun, Verma, Ashish, & Sooraj, KP (2024b). Quasi-stochastic departure metering model considering non-deterministic taxi time, standard instrument departure track time, and a new delay–Conflict relationship.” transportation research record. *Journal of the Transportation Research Board* April. 10.1177/03611981241240761.

Chandra, Aitichya, Verma, Ashish, Sooraj, K. P., Kunnathu, Nithya Parayam, & Padhi, Radhakant (2022). Understanding the terminal area traffic flow characteristics using flight record data. *Transportation in Developing Economies, 8*(2) Springer International Publishing. 10.1007/s40890-022-00153-8.

Chandra, Aitichya, Verma, Ashish, Sooraj, K. P., & Padhi, Radhakant (2023). Modelling and assessment of the arrival and departure process at the terminal area: A case study of Chennai International Airport. *Physica A: Statistical Mechanics and Its Applications, 615*(April), Article 128590. 10.1016/j.physa.2023.128590.

Chen, Dan, Hu, Minghua, Ma, Yuanyuan, & Yin, Jianan (2016). A Network-Based Dynamic Air Traffic Flow Model for Short-Term En Route Traffic Prediction. *Journal of Advanced Transportation, 50*(8), 2174–2192. 10.1002/atr.1453.

Chen, Dan, Hu, Minghua, Zhang, Honghai, Yin, Jianan, & Han, Ke (2017). A network based dynamic air traffic flow model for En route airspace system traffic flow optimization. *Transportation Research Part E: Logistics and Transportation Review, 106*(October), 1–19 Elsevier Ltd. 10.1016/j.tre.2017.07.009.

Chen, Yangzhou, Bi, Hong, Zhang, Defu, & Song, Zhuoxi (2013). Dynamic Airspace Sectorization via Improved Genetic Algorithm. *Journal of Modern Transportation, 21*(2), 117–124. 10.1007/s40534-013-0010-2.

Chen, Yangzhou, & Zhang, Defu (2014). Dynamic airspace configuration method based on a weighted graph model. *Chinese Journal of Aeronautics, 27*(4), 903–912. 10.1016/j.cja.2014.06.009.

Dai, Weibin, Zhang, Jun, Delahaye, Daniel, & Sun, Xiaoqian (2019). A Heuristic Algorithm for Aircraft 4D Trajectory Optimization Based on Bezier Curve.”. *13th USA/Europe Air Traffic Management Research and Development Seminar 2019*.

Delahaye, D., Alliot, J.-M., Schoenauer, M., & Farges, J.-L. (1994). Genetic algorithms for partitioning air space. In *Proceedings of the Tenth Conference on Artificial Intelligence for Applications* (pp. 291–297). IEEE. 10.1109/CAIA.1994.323662.

Edited by Kim, Sangkwon, Lee, Chaeyoung, Park, Jintae, Yoon, Sungha, Choi, Yongho, & Kim, Junseok (2021). A simple visualization method for three-dimensional (3D) network. *Discrete Dynamics in Nature and Society, 2021*(May), 1–10. 10.1155/2021/1426212.

Evler, Jan, Asadi, Ehsan, Preis, Henning, & Fricke, Hartmut (2021). Airline Ground Operations: Optimal Schedule Recovery with Uncertain Arrival Times. *Journal of Air Transport Management, 92*, Article 102021 Elsevier Ltd. 10.1016/j.jairtraman.2021.102021.

Fan, Yingsheng, Qi, Xiaogang, Li, Bo, & Liu, Lifang (2020). Fast clustering-based multidimensional scaling for mobile networks localisation. *IET Communications, 14*(1), 135–143. 10.1049/iet-com.2019.0444.

Flener, Pierre, and Justin Pearson. 2013. “Automatic airspace sectorisation: A survey,” November, 1–19. http://arxiv.org/abs/1311.0653.

Gardi, Alessandro, Sabatini, Roberto, & Kistan, Trevor (2019). Multi-objective 4D trajectory optimization for integrated avionics and air traffic management systems. *IEEE Transactions on Aerospace and Electronic Systems, 55*(1), 170–181 IEEE. 10.1109/TAES.2018.2849238.

Gerdes, Ingrid, Temme, Annette, & Schultz, Michael (2016). Dynamic airspace sectorization using controller task load. In *6th SESAR Innovation Days* (pp. 1–10).

Gianazza, David. (2017). Analysis of a workload model learned from past sector operations. In *7th SESAR Innovation Days* (pp. 1–10).

Gong, Maoguo, Cai, Qing, Chen, Xiaowei, & Ma, Lijia (2014). Complex network clustering by multi-objective discrete particle swarm optimization based on decomposition. *IEEE Transactions on Evolutionary Computation, 18*(1), 82–97 IEEE. 10.1109/TEVC.2013.2260862.

Gong, Maoguo, Cai, Qing, Li, Yangyang, & Ma, Jingjing (2012). An improved memetic algorithm for community detection in complex networks. In *2012 IEEE Congress on Evolutionary Computation, CEC 2012* (pp. 10–15). IEEE. 10.1109/CEC.2012.6252971.

Gong, Maoguo, Ma, Lijia, Zhang, Qingfu, & Jiao, Licheng (2012). Community detection in networks by using multi-objective evolutionary algorithm with decomposition. *Physica A: Statistical Mechanics and Its Applications, 391*(15), 4050–4060. 10.1016/j.physa.2012.03.021.

Guan, Xiangmin, Zhang, Xuejun, Lv, Renli, Chen, Jun, & Michal, Weiszer (2017). A Large-Scale Multi-Objective Flights Conflict Avoidance Approach Supporting 4D Trajectory Operation. *Science China Information Sciences, 60*(11), 1–13. 10.1007/s11432-016-9024-y.

Hind, Hassini, Amina, El Omri, Noreddine, Abghour, Khalid, Moussaid, & Mohammed, Rida (2018). Dynamic airspace configuration: review and open research issues. In *2018 4th International Conference on Logistics Operations Management (GOL)* (pp. 1–7). IEEE. 10.1109/GOL.2018.8378093.

Hossain, Md Murad, & Alam, Sameer (2017). A complex network approach towards modeling and analysis of the Australian airport network. *Journal of Air Transport Management, 60*, 1–9. 10.1016/j.jairtraman.2016.12.008.

Huber, Hans. (2018). India's Air Traffic: Towards an Empirical Framework for Systems Analysis. *Transportation Planning and Technology, 41*(6), 644–659 Taylor & Francis. 10.1080/03081060.2018.1488931.

IATA. 2023. "Global outlook for air transport a local sweet spot," no. December: 1–24.

Jagare, Peter, Flener, Pierre, & Pearson, Justin (2013). Airspace sectorisation using constraint-based local search. In *Proceedings of the 10th USA/Europe Air Traffic Management Research and Development Seminar, ATM 2013*.

Jakšić, Zoran, & Janić, Milan (2020). Modeling resilience of the ATC (air traffic control) sectors. *Journal of Air Transport Management, 89*(July). 10.1016/j.jairtraman.2020.101891.

Janić, Milan. (1997). A model of air traffic control sector capacity based on air traffic controller workload. *Transportation Planning and Technology, 20*(4), 311–335. 10.1080/03081069708717596.

Juntama, Paveen. (2022). Large Scale Adaptive 4D Trajectory Planning. *Uni- Versité Paul Sabatier - Toulouse III*. https://theses.hal.science/tel-04007919.

Koen, van de Merwe, Esther, Oprins, Fredrik, Eriksson, & Akos, van der Plaat (2012). The influence of automation support on performance, workload, and situation awareness of air traffic controllers. *The International Journal of Aviation Psychology, 22*(2), 120–143. 10.1080/10508414.2012.663241.

Kopardekar, Parimal, Bilimoria, Karl, & Sridhar, Banavar (2007). Initial Concepts for dynamic airspace configuration. In *7th AIAA ATIO Conf, 2nd CEIAT Int'l Conf on Innov and Integr in Aero Sciences,17th LTA Systems Tech Conf; Followed by 2nd TEOS Forum: 1* (pp. 695–706). Reston, Virigina: American Institute of Aeronautics and Astronautics. 10.2514/6.2007-7763.

Kulkarni, Sameer, Ganesan, Rajesh, & Sherry, Lance (2011). Static sectorization approach to dynamic airspace configuration using approximate dynamic programming. In *2011 Integrated Communications, Navigation, and Surveillance Conference Proceedings* (p. J2-1-J2-9). IEEE. 10.1109/ICNSURV.2011.5935295.

Lee, Paul, Prevot, Thomas, Homola, Jeffrey, Lee, Hwasoo, Kessell, Angela, & Smith, Nancy (2010). Sector design and boundary change considerations for flexible airspace management. In *10th AIAA Aviation Technology, Integration, and Operations (ATIO) Conference* (pp. 1–11). Reston, Virigina: American Institute of Aeronautics and Astronautics. 10.2514/6.2010-9376.

Leiden, Kenneth, Peters, Steven, & Quesada, Stacey (2009). Flight level-based dynamic airspace configuration. *9th AIAA Aviation Technology, Integration, and Operations Conference (ATIO)*. Reston, Virigina: American Institute of Aeronautics and Astronautics. 10.2514/6.2009-7104.

Li, Jinhua, Wang, Tong, Hwang, Inseok, & Hwang, Inseok (2009). A Spectral Clustering Based Algorithm for Dynamic Airspace Configuration. In *9th AIAA Aviation Technology, Integration, and Operations Conference (ATIO)* (pp. 1–21). Reston, Virigina: American Institute of Aeronautics and Astronautics. 10.2514/6.2009-7056.

Li, Jinhua, Wang, Tong, Savai, Mehernaz, & Hwang, Inseok (2010). Graph-based algorithm for dynamic airspace configuration. *Journal of Guidance, Control, and Dynamics, 33*(4), 1082–1094. 10.2514/1.47720.

Liu, Chengliang, Wang, Bangjuan, & Zhang, Hong (2023). Mapping the Spatial Organisation of Air Transport Network by WENA-MLST Analysis. *Transportmetrica A: Transport Science*, 1–26 September. 10.1080/23249935.2023.2261044.

Martínez, L Miguel (2006). TAZ delineation and information loss in transportation planning studies. *Master Thesis*.

Martinez, L, Viegas, Jose, & Silva, Elisabete (2007). Zoning decisions in transport planning and their impact on the precision of results. *Transportation Research Record: Journal of the Transportation Research Board, 1994*(1), 58–65.

Milan, Janić. (1989). Terminal area capacity model—A problem concerning air traffic controller workload. *Transportation Planning and Technology, 13*(3), 205–216. 10.1080/03081068908717400.

Mogtit, Abdessamed, Aribi, Noureddine, Lebbah, Yahia, & Lagha, Mohand (2020). Equitable Optimized Airspace Sectorization Based on Constraint Programming and OWA Aggregation. *Aircraft Engineering and Aerospace Technology, 92*(8), 1225–1243. 10.1108/AEAT-04-2019-0080.

Openshaw, S. (1977). A Geographical Solution to Scale and Aggregation Problems in Region-Building, Partitioning and Spatial Modelling. *Transactions of the Institute of British Geographers, 2*(4), 459–472. 10.2307/622300.

Openshaw, S. (1978). An empirical study of some zone-design criteria. *Environment and Planning A, 10*, 781–794. 10.1068/a100781.

Papadakis, Harris, Panagiotakis, Costas, & Fragopoulou, Paraskevi (2013). A Distributed Algorithm for Community Detection in Large Graphs. In *Proceedings of the 2013 IEEE/ACM International Conference on Advances in Social Networks Analysis and Mining* (pp. 1432–1434). New York, NY, USA: ACM. 10.1145/2492517.2492578.

Pien, Kuang-Chang, Han, Ke, Shang, Wenlong, Majumdar, Arnab, & Ochieng, Washington (2015). Robustness analysis of the European air traffic network. *Transportmetrica A: Transport Science, 11*(9), 772–792. 10.1080/23249935.2015.1087233.

PwC. 2022. "India: Emergence of a Global Leader in Aviation Knowledge Report on the Indian Aviation Industry," no. March.

Requião da Cunha, Bruno, Juan Carlos González-Avella, and Sebastián Gonçalves. 2015. "Fast fragmentation of networks using module-based attacks." Edited by Francisco J. Esteban. *PLOS ONE* 10 (11): e0142824. doi:10.1371/journal.pone.0142824.

Rosenow, Judith, Chen, Gong, Fricke, Hartmut, Sun, Xiaoqian, & Wang, Yanjun (2021). Impact of Chinese and European airspace constraints on trajectory optimization. *Aerospace, 8*(11), 338. 10.3390/aerospace8110338.

Sáez, Raúl, Prats, Xavier, Polishchuk, Tatiana, & Polishchuk, Valentin (2020). Traffic synchronization in terminal airspace to enable continuous descent operations in trombone sequencing and merging procedures: An implementation study for frankfurt airport. *Transportation Research Part C: Emerging Technologies, 121*(October). 10.1016/j.trc.2020.102875.

Savai, Mehernaz, Wei, Jian, Li, Jinhua, Wang, Tong, & Hwang, Inseok (2010). Multilevel graph partitioning algorithm for dynamic airspace configuration. In *10th AIAA Aviation Technology, Integration, and Operations (ATIO) Conference: 3* (pp. 1–8). Reston, Virigina: American Institute of Aeronautics and Astronautics. 10.2514/6.2010-9298.

Sergeeva, Marina, Delahaye, Daniel, Mancel, Catherine, & Vidosavljevic, Andrija (2017). Dynamic airspace configuration by genetic algorithm. *Journal of Traffic and Transportation Engineering (English Edition), 4*(3), 300–314 Elsevier Ltd. 10.1016/j.jtte.2017.05.002.

Sergeeva, Marina, Delahaye, Daniel, Mancel, Catherine, Zerrouki, Leila, & Schede, Nick (2015). 3D sectors design by genetic algorithm towards automated sectorisation. In *5th SESAR Innovation Days* (pp. 1–9).

Shahriari, Siroos, Ghasri, Milad, Sisson, S. A., & Rashidi, Taha (2020). Ensemble of ARIMA: Combining parametric and bootstrapping technique for traffic flow prediction. *Transportmetrica A: Transport Science, 16*(3), 1552–1573. 10.1080/23249935.2020.1764662.

Sherali, Hanif D, & Hill, Justin M (2013). Configuration of airspace sectors for balancing air traffic controller workload. *Annals of Operations Research, 203*(1), 3–31. 10.1007/s10479-011-0837-z.

Sun, Xiaoqian, & Wandelt, Sebastian (2021). Robustness of air transportation as complex networks: Systematic review of 15 years of research and outlook into the future. *Sustainability, 13*(11), 6446. 10.3390/su13116446.

Sun, Xiaoqian, Wandelt, Sebastian, & Zanin, Massimiliano (2017). Worldwide air transportation networks: A matter of scale and fractality? *Transportmetrica A: Transport Science, 13*(7), 607–630. 10.1080/23249935.2017.1312632.

Tang, Jiangjun, Alam, Sameer, Lokan, Chris, & Abbass, Hussein A. (2012). A Multi-Objective Approach for Dynamic Airspace Sectorization Using Agent Based and Geometric Models. *Transportation Research Part C: Emerging Technologies, 21*(1), 89–121 Elsevier Ltd. 10.1016/j.trc.2011.08.008.

Teixeira, Inˆes S.F. Salavisa. 2015. "Optimization of airspace sectorization in ATM," 1–10.

Todorov, T D, & Simeonov, S (2020). Optimal Sector Modelling of Airspace Based on Optimization Algorithms. *IOP Conference Series: Materials Science and Engineering, 1002*(1), Article 012004. 10.1088/1757-899X/1002/1/012004.

Treimuth, Tambet, Delahaye, Daniel, & Ngueveu, Sandra Ulrich (2016). A Branch-and-price algorithm for dynamic sector configuration. In *8th International Conference on Applied Operational Research (ICAOR), Jun 2016, Rotterdam, Netherlands* (pp. 47–53).

Wandelt, Sebastian, Shi, Xing, & Sun, Xiaoqian (2021). Estimation and improvement of transportation network robustness by exploiting communities. *Reliability Engineering & System Safety, 206*(November 2020), Article 107307 Elsevier Ltd. 10.1016/j.ress.2020.107307.

Wandelt, Sebastian, & Sun, Xiaoqian (2014). Efficient compression of 4D-trajectory data in air traffic management. *IEEE Transactions on Intelligent Transportation Systems, 16*(2), 1–10 IEEE. 10.1109/TITS.2014.2345055.

Wang, Jiaoe, Mo, Huihui, Wang, Fahui, & Jin, Fengjun (2011). Exploring the network structure and nodal centrality of China's air transport network: A complex network approach. *Journal of Transport Geography, 19*(4), 712–721 Elsevier Ltd. 10.1016/j.jtrangeo.2010.08.012.

Xue, Min. (2009). Airspace sector redesign based on voronoi diagrams. *Journal of Aerospace Computing, Information, and Communication, 6*(12), 624–634. 10.2514/1.41159.

Xue, Min. (2010). Three Dimensional Sector Design with Optimal Number of Sectors. *AIAA Guidance, Navigation, and Control Conference*. Reston, Virigina: American Institute of Aeronautics and Astronautics. 10.2514/6.2010-8290.

Yang, Lei, Huang, Jue, Gao, Qi, Zhou, Yi, Hu, Minghua, & Xie, Hua (2022). Dynamic boundary optimization of free route airspace sectors. *Aerospace, 9*(12), 832. 10.3390/aerospace9120832.

Yin, Cheryl Wong Sze, Venugopalan, T. K., & Suresh, S. (2017). A Multi-Objective approach for 3D airspace sectorization: A study on singapore regional airspace. *2016 IEEE Symposium Series on Computational Intelligence, SSCI 2016*. IEEE. 10.1109/SSCI.2016.7850098.

Yousefi, Arash. (2005). Optimum airspace design with air traffic controller workload-based partitioning. *George Mason University*. https://www.library.northwestern.edu/find-borrow-request/requests-interlibrary-loan/lending-institutions.html.

Zeh, Thomas, Rosenow, Judith, Lindner, Martin, & Stanley, F (2024). Trajectory and airspace optimization depending on controller task load. *ICRAT 2024*.

Zou, Xiang, Cheng, Peng, An, Bang, & Song, Jingyan (2016). Sectorization and Configuration Transition in Airspace Design. *Mathematical Problems in Engineering, 2016*(i). 10.1155/2016/6048326.